UNIVERSITY OF CALIFORNIA, BERKELEY

BERKELEY • DAVIS • IRVINE • LOS ANGELES • RIVERSIDE • SAN DIEGO • SAN FRANCISCO SANTA BARBARA • SANTA CRUZ

SEISMOGRAPHIC STATION
DEPARTMENT OF GEOLOGY AND GEOPHYSICS

BERKELEY, CALIFORNIA 94720

29 December 1980

Director, ARPA
1400 Wilson Boulevard
Arlington, Virginia 22209

Attn: Program Management

TECHNICAL REPORTS 5 - 8, 01 Oct 1979 - 30 Sep 1980

ARPA Order No. 3291-21
Program Code 9F10
Grantee: The Regents of the University of California
Effective Date of Grant: 01 October 1978
Grant Termination Date: 30 Septermber 1980
Amount of Grant: $102,520
Grant No. AFOSR-F49620-79-C-0028
Principal Investigators: T. V. McEvilly (415)642-4494
L. R. Johnson (415)642-1275
Program Manager: William J. Best (202)693-0162

Short Title of Work: BROADBAND DISCRIMINATION STUDIES

T. V. McEvilly

L. R. Johnson

Sponsored by
Advanced Research Projects Agency (DOD)
ARPA Order No. 3291
Monitored by AFOSR Under Contract No. F49620-79-C-0028

TABLE OF CONTENTS

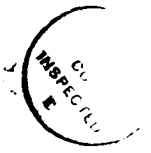

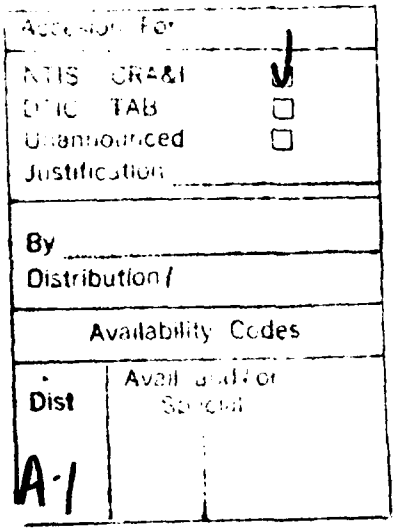

SECURITY CLASSIFICATION OF THIS PAGE *(When Data Entered)*

REPORT DOCUMENTATION PAGE		READ INSTRUCTIONS BEFORE COMPLETING FORM
1. REPORT NUMBER Technical Reports 5-8	2. GOVT ACCESSION NO.	3. RECIPIENT'S CATALOG NUMBER
4. TITLE *(and Subtitle)* Broadband Discrimination Studies		5. TYPE OF REPORT & PERIOD COVERED Technical Reports 5-8 01 Oct 1979-30 Sep 1980
		6 PERFORMING ORG. REPORT NUMBER
7. AUTHOR(s) T. V. McEvilly L. R. Johnson		8. CONTRACT OR GRANT NUMBER(s) AFOSR-F$(¢@)-79-C-0028
9. PERFORMING ORGANIZATION NAME AND ADDRESS Seismographic Station University of California Berkeley, California 94720		10. PROGRAM ELEMENT, PROJECT, TASK AREA & WORK UNIT NUMBERS AO 3291-21 9D60 61101F
11. CONTROLLING OFFICE NAME AND ADDRESS ARPA 1400 Wilson Boulevard Arlington, Virginia 22209		12. REPORT DATE 29 Dec 1980
		13. NUMBER OF PAGES 73
14. MONITORING AGENCY NAME & ADDRESS*(if different from Controlling Office)* AFOSR Bolling Air Force Base Washington, D.C. 20332		15. SECURITY CLASS. *(of this report)* Unclassified
		15a. DECLASSIFICATION/DOWNGRADING SCHEDULE

16. DISTRIBUTION STATEMENT *(of this Report)*

Approved for public release; distribution unlimited.

17. DISTRIBUTION STATEMENT *(of the abstract entered in Block 20, if different from Report)*

18. SUPPLEMENTARY NOTES

19. KEY WORDS *(Continue on reverse side if necessary and identify by block number)*

nuclear explosions	scattering
seismic data	seismic surface waves
seismic array	dispersion
spatial coherence	phase-matched filter

20. ABSTRACT *(Continue on reverse side if necessary and identify by block number)*

In the course of our previous studies of elastic waves generated by nuclear explosions, a number of questions have arisen which are difficult to answer through the analysis of data from individual seismic stations. The direction of approach of various phases, their apparent velocity, and the degree of their spatial coherence are all matters which are not completely understood for data recorded at small distances from explosions.

DD FORM 1 JAN 73 1473

SECURITY CLASSIFICATION OF THIS PAGE *(When Data Entered)*

This lack of understanding hinders the interpretation of the data and the study of the explosive source mechanism. Such considerations have led us to use a small array of seismic stations to record the elastic wave field from a number of explosions.

A seismic array consisting of 9 stations arranged as three nested triangles with minimum spacing of 100 m and maximum spacing of 400 m was used to record the two NTS explosions, LIPTAUER in Yucca Valley on 3 April 1980 and COLWICK on Pahute Mesa on 26 April 1980. The distance of the array from the explosion was 1.9 km for LIPTAUER and 6.0 km for COLWICK.

So far our analysis has concentrated on the COLWICK data. Preliminary results show that most of the energy in the first 5 sec of the seismograms is propagating at an azimuth and velocity which are consistent with generation at or very near the explosive source. The spatial coherence decays by a factor of $1/e$ at distances that range between 400 and 1200 m, depending upon direction and component of motion. In a direction parallel to the wavefront, the vertical and radial components are much more coherent than the transverse component, while all of the components have comparable coherence in a direction perpendicular to the wavefront. Coherence generally decreases as frequency increases.

In addition to aiding our interpretation of elastic waves generated by an explosion, these array data should provide useful constraints on the possible mechanisms by which elastic waves can be scattered by inhomogeneities near the surface of the earth.

A large body of surface wave data recorded at regional distances in the California-Nevada region is being analysed to obtain estimates of velocity and attenuation in the crust. The observed surface waves require a considerable amount of processing in order to extract the necessary information. Both the phase-matched filter and moving-window analysis schemes have been used with the former proving to be superior. It appears that excellent dispersion and amplitude data can be extracted from the seismograms in the period range 5 to 50 sec.

For the sake of completeness, a report is included which was prepared in response to a specific DARPA request. This report is a review of "Near-source effects on P waves".

A catalog of digital data has been assembled which contains much of the data collected and analysed in DARPA supported research of previous years. A preliminary version of the catalog index for the period 1965-1971 is included in this report.

than the transverse component, while all of the components have comparable coherence in a direction perpendicular to the wavefront. Coherence generally decreases as frequency increases.

In addition to aiding our interpretation of elastic waves generated by an explosion, these array data should provide useful constraints on the possible mechanisms by which elastic waves can be scattered by inhomogeneities near the surface of the earth.

A large body of surface wave data recorded at regional distances in the California-Nevada region is being analysed to obtain estimates of velocity and attenuation in the crust. The observed surface waves require a considerable amount of processing in order to extract the necessary information. Both the phase-matched filter and moving-window analysis schemes have been used with the former proving to be superior. It appears that excellent dispersion and amplitude data can be extracted from the seismograms in the period range 5 to 50 sec.

For the sake of completness, a report is included which was prepared in response to a specific DARPA request. This report is a review of "Near-source effects on P waves".

A catalog of digital data has been assembled which contains much of the data collected and analysed in DARPA supported research of previous years. A preliminary version of the catalog index for the period 1965-1971 is included in this report.

1. Summary

In the course of our previous studies of elastic waves generated by nuclear explosions, a number of questions have arisen which are difficult to answer through the analysis of data from individual seismic stations. The direction of approach of various phases, their apparent velocity, and the degree of their spatial coherence are all matters which are not completely understood for data recorded at small distances from explosions. This lack of understanding hinders the interpretation of the data and the study of the explosive source mechanism. Such considerations have led us to use a small array of seismic stations to record the elastic wave field from a number of explosions.

A seismic array consisting of 9 stations arranged as three nested triangles with minimum spacing of 100 m and maximum spacing of 400 m was used to record the two NTS explosions, LIPTAUER in Yucca Valley on 3 April 1980 and COLWICK on Pahute Mesa on 26 April 1980. The distance of the array from the explosion was 1.9 km for LIPTAUER and 6.0 km for COLWICK.

So far our analysis has concentrated on the COLWICK data. Preliminary results show that most of the energy in the first 5 sec of the seismograms is propagating at an azimuth and velocity which are consistent with generation at or very near the explosive source. The spatial coherence decays by a factor of e^{-1} at distances that range between 400 and 1200 m, depending upon direction and component of motion. In a direction parallel to the wavefront, the vertical and radial components are much more coherent

II. Near field array studies

Motivation

From Pahute Mesa NTS explosions anomalous features in the near field accelerograms have been noticed in previous field experiments. Significant transverse accelerations are observed coincident with the initial P wave arrival. It was not clear whether this transverse motion was coherent for any considerable areal extent,or was confined to localized sites. Our previous experiments with widely spaced stations were not suitable to answer this question. The energy of the transverse seismogram is comparable to the vertical seismogram and transverse peak accelerations often exceed the vertical or radial peak accelerations. Due to the sensitivty of the transverse components to a deviatoric (non-explosive) source component, it was desirable to understand the nature of the waves propagating with an apparent transverse component, and to test the hypothesis that large transverse motions were due to off-azimuth SV waves as opposed to on-azimuth SH waves.

Design

A small array of closely spaced,broadband, large dynamic range, three-component accelerometers was considered to address the questions on spatial coherence and wave properties. As with previous experiments, digital event recorders with three-component packages of force-balanced servo-accelerometers were used. Ideally, we needed to measure, 1. direction of arrival, 2. apparent velocity and, 3. spatial coherence. The array had to be easily and quickly deployed, to be fault tolerant, to be limited to nine stations, to afford common timing and to preclude spatial aliasing while providing sufficient resolution in two dimensional slowness space. A nested set of three triangles was selected.

Deployment was made for two shots, Liptauer and Colwick at 1.9 and 6.0 kilometers respectively. Liptauer was an equivalent local magnitude 4.7 explosion located in Yucca Valley. Colwick was an equivalent local magnitude 5.5 explosion on Pahute Mesa. At Liptauer a common triggering of the array was attempted to provide relative timing. At Colwick all event recorders were allowed to trigger individually and all records were time shifted assuming a given P wave velocity. At each site one out of nine recorders malfunctioned, leaving eight stations arranged as in Figures 2 and 3. The wave number impulse responses are shown in Figures 4,and 5. Resolution, for each array, was about 1 cycle/km at half maximum response and the spatial Nyquist wavenumber was about 6 cycles/km in all directions. It was possible to make crude slowness spectral estimates in the 1 to 4 Hertz band. The spatial decay of coherence could be observed in the longitudinal as well as the transverse

directions. For any frequency band the rate at which coherence between stations decays with increasing separation could be measured in two dimension.

Deployment of the array required four to six man days to survey, implace, and test. Removal of the equipment required between one and two man days, less travelling. The arrays were deployed with in a week prior to the event and external power was provided by automobile twelve volt batteries with sufficient amp-hours to power the accelerometers and digital event recorders for one week. Common triggering required laying a twisted pair of wires between stations to provide a common slave signal. The trigger signal logic required three simultaneous trigger signals from three of the nine event recorders. Aproximately one half second of pre-event memory was availible at 200 samples per second for all three components. Records are roughly fifty seconds long. Antialias filters were either at 25 or 50 hertz.

Liptauer

The traces from the Liptauer array are seen in Figures 6, 7,and 8. The ratio of the vertical to radial amplitudes for both P and S waves and the short duration of the seismograms suggest a half space model may fit the data well. The largest peak transverse signal rivals the radial component and often exceeds it at individual stations. The large transverse pulse at 1.7 sec is visually coherent. The slight emergent transverse motion coincident with the P wave is coherent as well.

Colwick

The traces from the Colwick array are seen in Figures 9, 10,and 11. The largest peak acceleration was 18+/-3 % g on the radial component. The large vertical-to-radial P wave ratio and radial-to-vertical S wave ratio suggest velocity gradients to increase the angles of incidence. The lengths and complexity of the seismograms also indicate that a more complicated structure may be necessary for Pahute Mesa than is needed for Yucca Valley. Visually, the Colwick seismograms show less coherence, possibly due to the presence of more high frequencies.

Processing

Programs were developed to perform most of the desired processing upon a captive minicomputer. The remainder of the computing was performed on a CDC 6400. The individual event recorder tapes are played into the minicomputer, the data are reformated and stored on disk and tape. Processing includes time domain stacking, spectra, high resolution and convential wave-number analysis, and cross-correlations. At present processing continues upon both data sets while the analysis for the Colwick array is more complete. Discussion will stress the results obtained to date from the Colwick array.

1. Stacking

From the wave number impulse responce we can estimate that the resolution of the Colwick array at 5 Hz is +/- 0.2 sec/km. Stacking of

the seismograms was done for slownesses from 1.2 to -1.2 sec/km at steps of 0.2 sec/km on azimuth with the shot. The results indicate that the majority of the coherent energy propogates from the shot at slownesses less than 1 sec/km and that the initial body waves all arrive with slownesses less than 0.25 sec/km, with respect to the initial P wave. Stacking of the seismograms can be seen to deemphasize the high frequencies. Unless these high frequencies propagate at significantly higher apparrent velocities, there must be a loss of coherency with increasing frequency. In an attempt to measure this phenomenon, filtered two-station cross-correlations were calculated. The results are presented in section 3. The large transverse pulse at 1.5 sec stacks up 0.2 sec/km slower than the P wave. Some later arrivals have been found to stack up for off azimuth slownesses. A stategy that has been useful for detecting scattered waves is to stack suspicious off-azimuth peaks that occur in the wave number spectra.

2. Wavenumber spectra

Windows were selected for the calculation of cross-spectra to compute slowness spectra at selected frequencies. Both conventional and "high resolution" methods were used. The beam forming or conventional method retains the dynamic range of the data but is cluttered by side lobe excitation. The partial removal of side lobes by the high resolution or maximum liklihood method is convienant for these arrays (Capon, Greenfield, and Kolker, 1967; Capon, 1969; and Capon, 1970).

The preliminary analysis of the Colwick and Liptauer array data show that coherent energy from the source azimuth is dominant on all three components for the first 5 seconds. In Figures 13, and 14 we see the Colwick array high resolution slowness spectra at 3.7 Hz for the first 5 seconds of data. The origin of the plots corresponds to the slowness of the initial P wave arrival. The convention is for the wave number vector to project in the direction from which the arrival comes. The shot was in the direction of the negative Y axis. The vertical component acceleration (Figure 13) shows a prominent peak 0.25 sec/km faster than the initial P wave and hence in the direction of the plus Y axis. This confirms the impression derived from time domain stacking that some body waves are very fast. The remainder of the energy in the vertical component is distributed at slownesses less than 0.7 sec/km with respect to the P wave on the azimuth of the source.

The large transverse pulses are not off-azimuth SV waves to within the resolution of the arrays. The large transverse pulse at 1.5 sec observed at the Colwick array coincides with a well defined peak in slowness space 0.2 sec/km slower than the P wave, as seen in Figure 14. This is consistent with propagation as a direct S wave from the source. The remainder of the coherent energy in the transverse component is distributed between 0.0 and 1.0 sec/km, with respect to the initial P wave, and on azimuth with the shot. During these first 5 seconds, the transverse component shows no indication of contamination by coherent arrivals faster than the initial P wave. Windows later in the records have revealed significantly off- and back-azimuth arrivals which stack up in the time domain as distinct arrivals. However, these scattered packets of energy are not observed when the first five seconds of data

are analyzed as a block.

3. Two-Station Cross-Correlations

Both time domain stacking and wavenumber analysis utilize the whole array and emphasize the coherent parts of the seismogram. In order to explore the incoherent part of the seismogram we formed two station cross-correlations. Out of eight stations we can make 28 pairs of stations. The Colwick array was arranged to order data into transversely and longitudinally separated station pairs. This provides a comparison of repeatable ground motion across a wave front as well as along the direction of propagation.

The cross-correlation function serves as an unbiased estimate of the spatial covariance (Weiner, 1949; Bretherton and McWilliams 1980). Furthermore, filtered cross-correlations yield information about the frequency dependence of coherence. Analysis of the spatial decay of coherence can serve to test theories of wave propagation in randomly heterogeneous media. Such formalisms for scalar wave propagation predict differences between longitudinal and transverse spatial covariance functions (Chernov 1960, Ishimaru 1979). Analysis has progressed in this direction for the Colwick array data. We have concentrated the processing upon the first 5 sec block of the data for a test of methodology.

The two-station cross-correlations for all three components were considered to be functions of station separation and separation direction. For stations i and j at locations r_i and r_j the cross-correlation, shown in Figure 15, was modeled as

$$R_{i,j}(r_i,r_j)=R_{i,j}(|x_i-x_j|,|y_i-y_j|)$$

In particular, a fair fit to the data was obtained by assuming a simple exponential decay.

$$R_{i,j}=\exp(-a_x|x_i-x_j|-a_y|y_i-y_j|)$$

With the x axis aligned in the transverse direction, and the y axis in the longitudinal direction. Because the array had only 13 independant pairs of $|x_i-x_j|,|y_i-y_j|$ out of 28 pairs of stations, consistency of the data could be examined. In Figure 16 we see the values of the data contoured by the fit to a_x,a_y for each component. The RMS residuals for the three components indicate a fair fit.

	$1.0/a_x$	$1.0/a_y$	rms residual
vertical	1465 meters	663 meters	.04
radial	1960	471	.07
transverse	429	477	.11

For comparison, the two station cross-correlations are plotted in Figure 17 versus the station separation. This one-dimensional

representation shows much scatter. We see three curves for each component. These represent cross sections through the two-dimensional surface that was fit to the data. For a perfect fit to the data these curves would span the the individual measurements plotted in Figure 17. The data suggest we can rank the components in increasing sensitivity to heterogeneity, for an explosion source, as vertical, radial, and transverse.

The loss of coherence along the wave front (transverse separaration) for the transverse component is of the same order as in the direction of propagation. The radial and vertical components show more coherence across the the wave front than in the dirction of propagation at the same separation. It must be noted that the loss of coherence in the longitudinal direction due to a changing deterministic seismogram with distance has not been removed. It must also be emphasized that this represents the whole of the first 5 seconds of data, including both coherent signal seen in the wave number spectra and incoherent energy that does not stack in beam forming. This incoherent energy can be considered a form of signal generated noise produced by an interaction of the geologic heterogeneity with the coherent waves propagating through an average homogeneous structure.

Additional information exists in the frequency dependence of coherence (Knopoff and Hudson, 1964 and 1967; Hudson and Knopoff, 1966; and Karal and Keller, 1964). Each component of ground motion contains scattered energy contributed by all modes of propogation. A source with small deviatoric part produces dominating radial and vertical components. The data suggest the incoherent portion of the transverse component of ground motion is dominated by scattered energy from the P and SV modes from the explosive source. The remaining transverse coherent energy is propagating SH waves from a small deviatoric source. Due to the larger initial excitation of the P and SV modes they contain ,on the average, proportionately less incoherent scattered waves. It has been shown (Knopoff and Hudson 1967) that the P-to-S and S-to-S conversions are dominant over P-to-P and S-to-P conversions. The P and SV modes of propagation will supply incoherent energy to the SH modes of propogation in much larger proportion than will the SH modes provide scattered energy to the P and SV modes of propogation. The resultant tendency will be for the incoherent fraction of the transverse component to be larger for the radial and vertical fractions of incoherent-to-coherent energy. Frequency dependance of the coherence for all three components will be helpful to estimate inhomogeneity in the medium.

An estimation of the frequency dependence of coherence was attempted by filtering the cross-correlation functions. Seven pairs of stations were selected that gave either purely transverse separation or purely longitudinal separation. In order to remove the frequency dependence of the source, the cross-spectra were normalized. The cross-spectra were then low-pass filtered at 2.5, 5.0, 10., and 20. hertz. The inverse Fourier transform was applied yielding a filtered cross-correlation. We see an example for stations 1 and 4 in Figure 18 . We can interpret the decreasing correlation with in increasing bandwidth as showing 91% of the bandwidth below 5 hertz is coherent while only 64% coherent below 20. hertz.

For the three components the maximum correlations are plotted in Figure 19 versus the corner frequency of the filter. The station pairs are separated into two populations purely transverse or purely longitudinal separations. All three components show a sharp fall-off with increasing corner frequency. Although the vertical and radial components show the two populations as separated, the transverse component can not distinguish between the two populations. Further analysis will include bandpass filtering of the cross-correlations as well as detailed analysis of selected shorter windows. The exact nature of the energy on the transverse component prior to the arrival of a causal S wave will require such a window.

Conclusions

The analysis of the Colwick array data is still incomplete, and much remains to be done with the Liptauer experiment data. Comparison of the two sites will be useful for a test of the methodology as well as a test of the two different geologic settings. Preliminary analysis for both arrays has demonstrated that a significant fraction of the transverse energy consists of propagating SH waves arriving at apparent velocities and times consistant with a deviatoric (non-explosive) component in the source region.

The arrays of closely spaced stations provide a means to investigate the spatial coherence of waves in a complex geologic setting. Our confidence in the use of accelerograms to study the source has been increased. The persistence of the coherent energy of the early waves arriving at the expected azimuth supports the use of laterally homogeneous Green's functions in source studies.

At the same time, the array data provide definition of the statistical coda contained in the seismogram. The sensitivity of the components of ground motion to lateral heterogeneity for these explosion sources has been measured. The radial and vertical components were found to have comparable amounts of incoherent energy increasing proportionately with frequency. The conerence along the wave front for these components was found to be excellent in a bandwidth up to 10 Hz at ranges exceeding the size of the arrays. The transverse component of the ground acceleration was found to differ from the other two components in the proportion of scattered energy. In terms of equivalent separation for a given loss in waveform coherence, a mislocation of 400 meters at 6 km in a transverse direction would affect the SH seismogram, by the same amount as would a similar positional error in the radial distance from the event. For radial or vertical seismograms, a mislocation in the radial direction of 400 meters would affect the seismogram the same amount as a positional error in the azimuthal direction of as much as 1.5 km. We may think of this incoherent energy as signal generated noise and treat it accordingly for the purposes of inversion procedures.

The remaining work to be done will require an estimate of the coherent-to-incoherent signal ratios for the various components in the appropriate geologic settings. This is in a very broad sense the determination of the statistics for the stochastic Green's function (Adomain 1964).

References

Adomain 1964, Stochastic Green's functions,Stochastic Processes in Mathematical Physics and Engineering, Proc. of Symp. in App. Math. v XVI,1-30.

Bretherton and Mcwilliams 1980, Estimation From Irregular Arrays, Reviews of Geophysics and Space Physics, v18, n4, 789-812.

Capon,Greenfield, and Kolker 1967, Multidimensional Maximum-likelihood Processing of a Large Aperture Seismic Array, Proc. IEEE v55, n2, Feb 67, 192-211.

Capon 1969, High Resolution Frequency Wave Number Spectrum Analysis, Proc. IEEE, v57, n8, Aug 69, 1408-18.

Capon 1970, Probabilty Distributions For Estimators of the Frequency Wave Number Spectrum, Proc. IEEE, v58, n10, Oct 70, 1785-6.

Chernov 1960, Wave Propagation in a Random Medium, Mcgraw-Hill.

Hudson and Knopoff 1966, The nature of Seismic Noise, Proc. Roy. Soc. Lon. A290, 290-296.

Karal and Keller 1964, Elastic,Electromagnetic and other Waves in a Random Medium, J. of Math. Phys. v5, n4, 537-47.

Knopoff and Hudsun 1964, Scattering of Elastic Waves by Small Inhomogeneities, J. Acoust. Soc. Am. v36, n2, 338-43.

Knopoff and Hudson 1967, Frequency Dependance of Amplitudes of Scattered Elastic Waves, J. Acoust. Soc. Am. v42, n1, 18-20

Ishimaru 1978, Wave Propagation and Scattering in Random Media, V I&II Academic Press.

Weiner,N. 1949, Time Series, Mit Press, 163pgs.

Figure Captions

Figure 1. Locations of the NTS explosions which were studied and the accelerometer arrays.

Figure 2. Arrangement of the accelerometer array for the explosion LIPTAUER.

Figure 3. Arrangement of the accelerometer array for the explosion COLWICK.

Figure 4. Wavenumber impulse response for the LIPTAUER array.

Figure 5. Wavenumber impulse response for the COLWICK array.

Figure 6, 7, 8. 13 sec of individual traces from the LIPTAUER array. Station numbers are on the left. The vertical bars are 0.1 g.

Figures 9, 10, 11. 5.5 sec of individual traces from the COLWICK array. Station numbers are on the left. The vertical bars are 0.1 g.

Figure 12. Averaged acceleration spectra from the first 5 sec at the COLWICK array.

Figure 13. High resolution vertical compoment acceleration wavenumber power spectra at 3.7 Hz for the first 5.12 sec of data. The origin corresponds to the slowness of the first arrival. The azimuth of the source is in the direction of the negative Y axis.

Figure 14. Similar to Figure 13 for the transverse component.

Figure 15. Example of a cross-correlation after normalization by the corresponding auto-correlations.

Figure 16. Contours of the spatial dependence of the maximum of the two-station cross-correlations. The dots represent the postions of the 13 independent data points which constrain the surface. Values at the data points are suppressed for clarity.

Figure 17. Spatial decay of the two-station cross-correlations. The curves represent sections through the surface of Figure 16: solid - direction of maximum gradient, short dashed - transverse direction, long short dashed - longitudinal direction.

Figure 18. Example of a normalized and low-pass filtered cross-correlation function at corner frequencies of 2.5, 5.0, 10.0, and 20.0 Hz.

Figure 19. Filtered cross-correlations versus corner frequency. Seven pairs of stations are presented, either pure transverse separation or pure longitudinal separation.

NEVADA TEST SITE

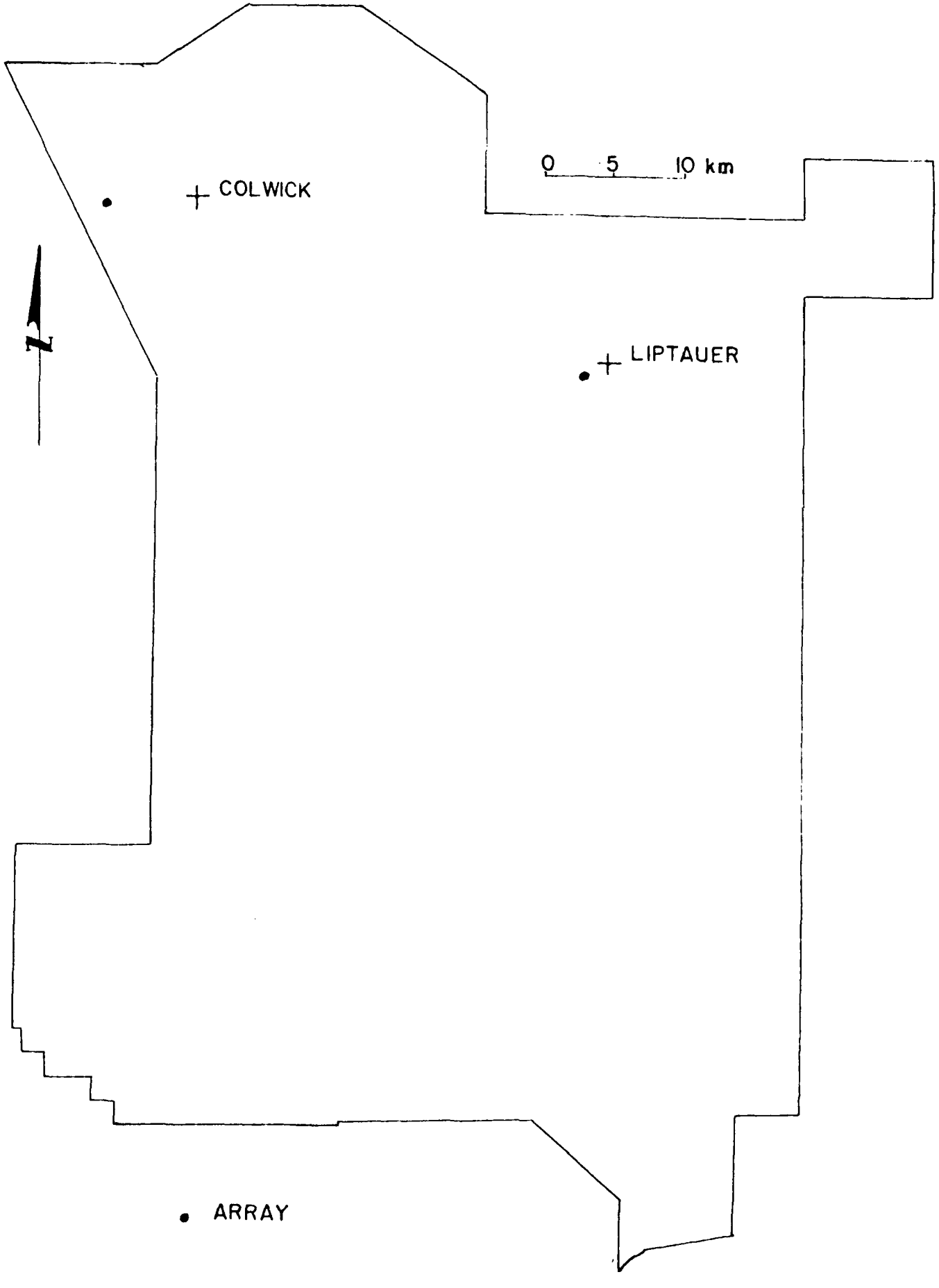

FIGURE 1

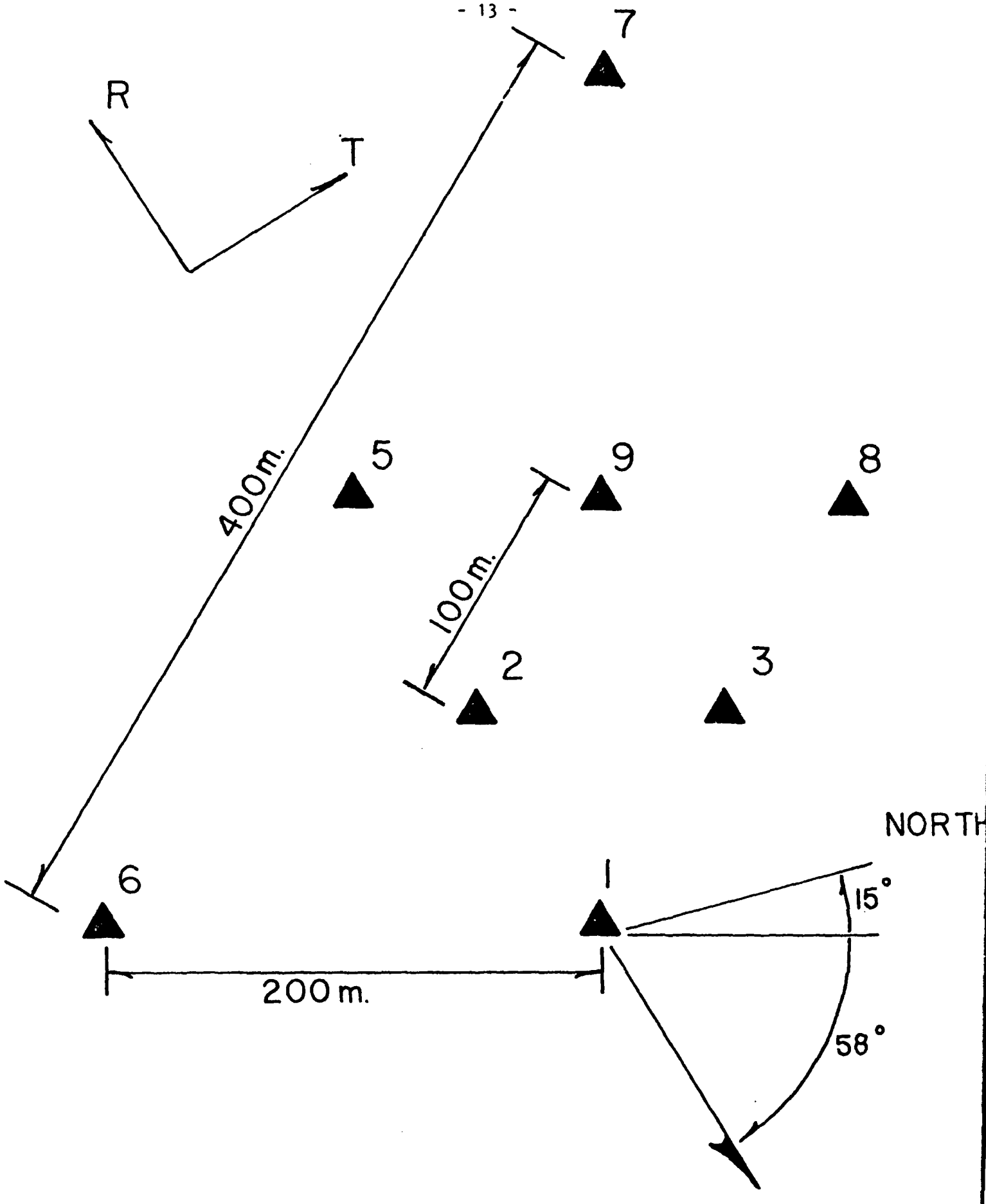

FIGURE 2

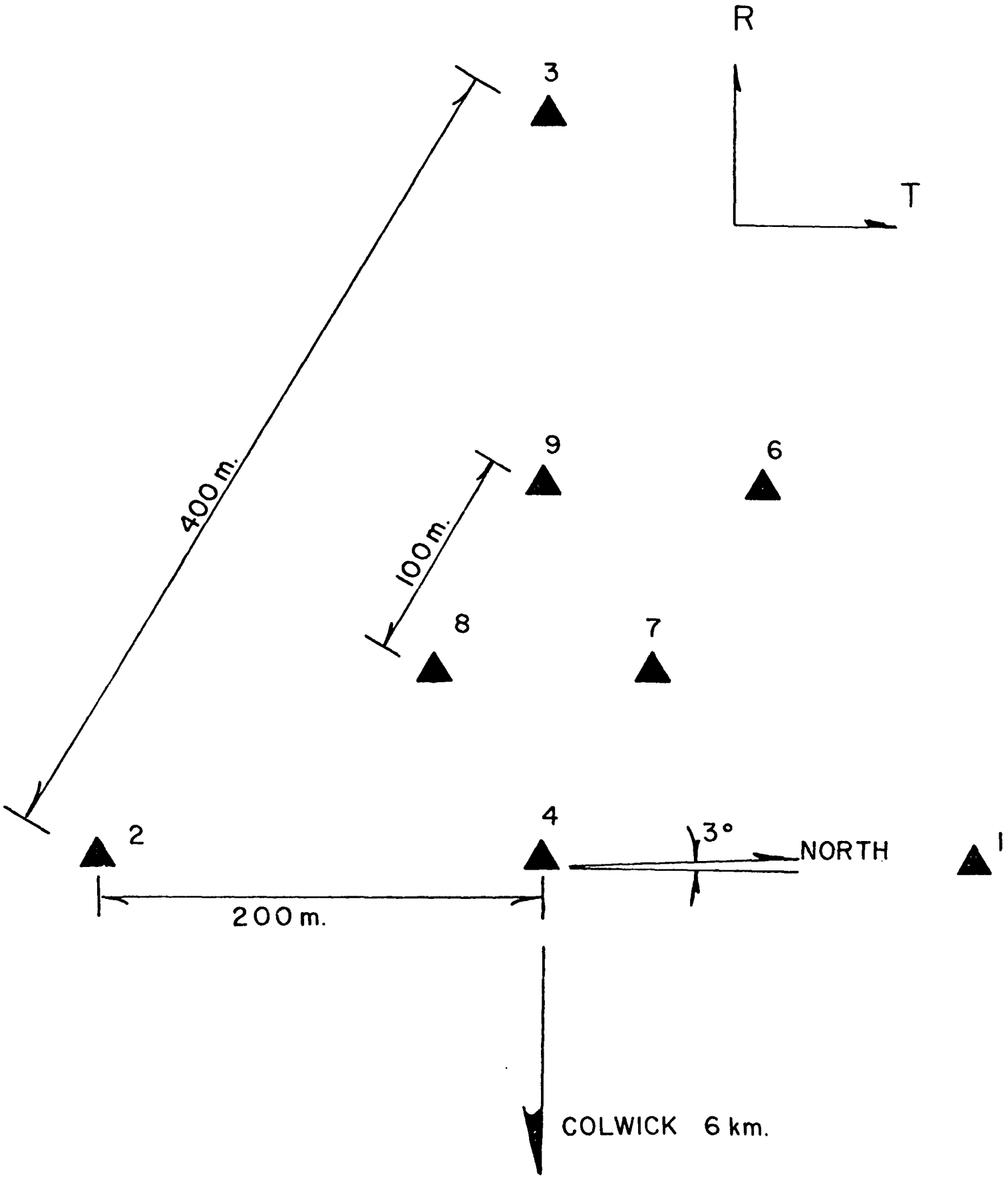

FIGURE 3

LIPTAUER ARRAY WAVENUMBER IMPULSE RESPONSE

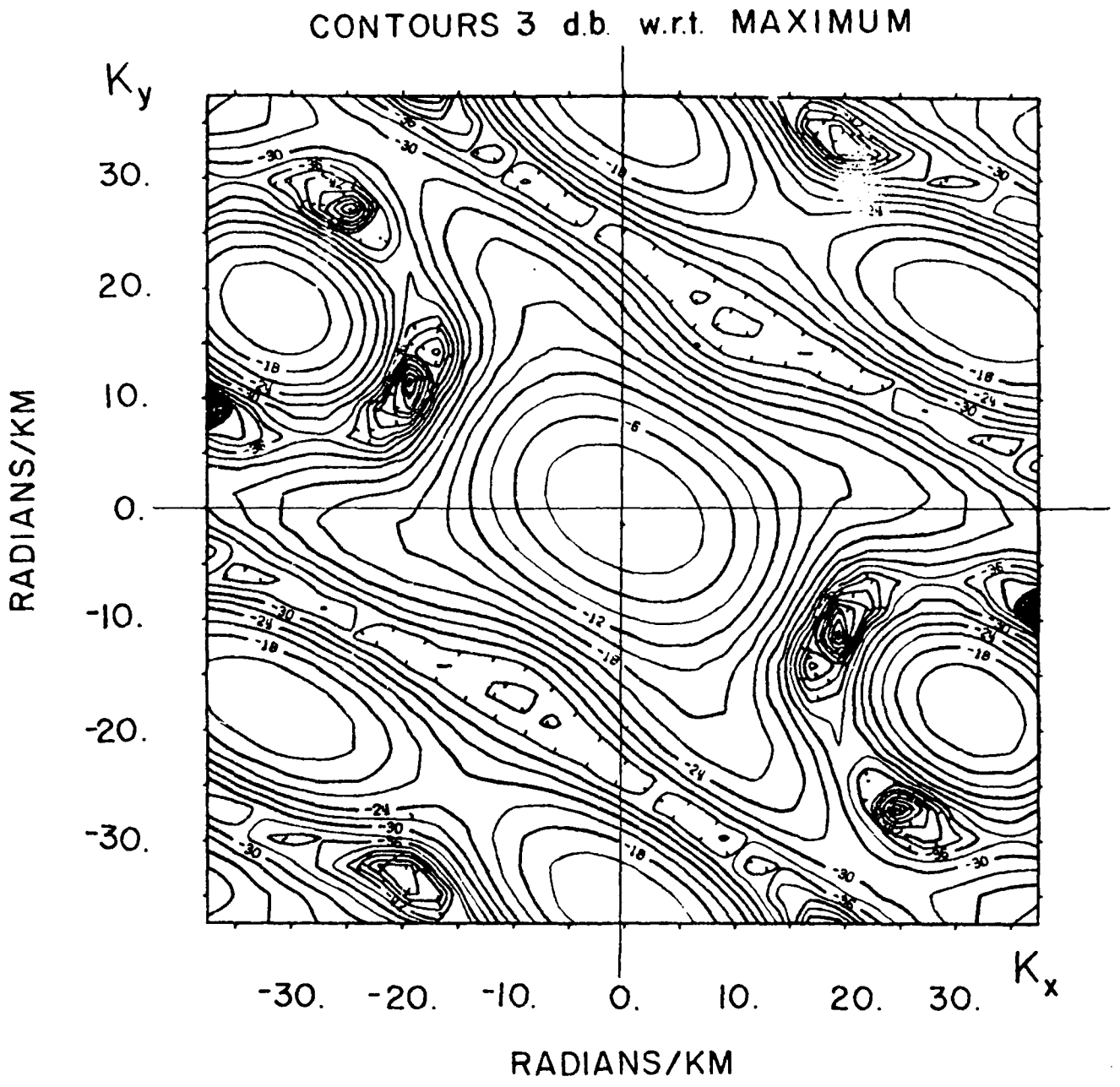

FIGURE 4

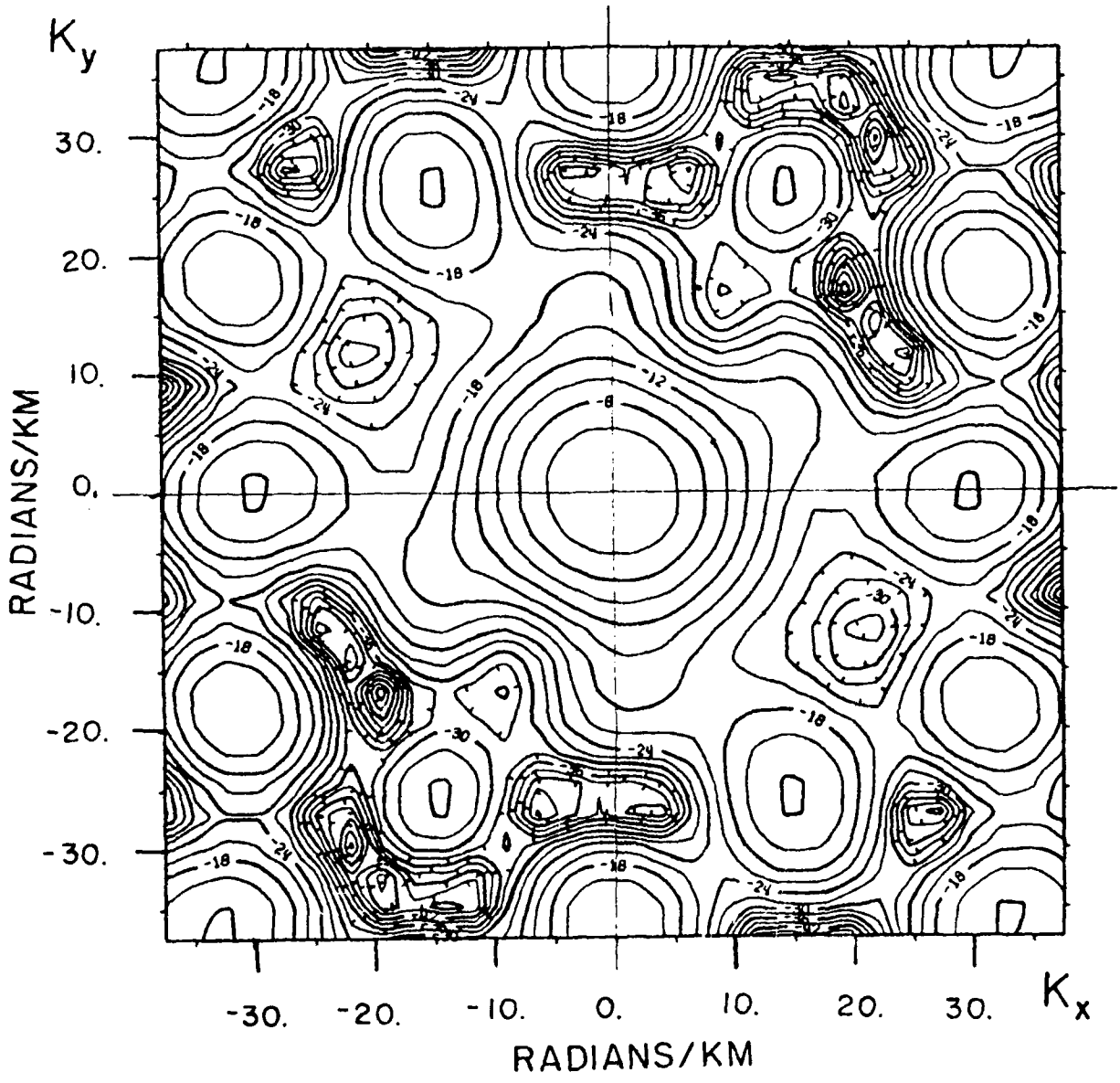
COLWICK ARRAY WAVENUMBER IMPULSE RESPONSE
CONTOURS 3 d.b. w.r.t. MAXIMUM
K_y
30.
20.
10.
0.
-10.
-20.
-30.
RADIANS/KM
-30.
-20.
-10.
0.
10.
20.
30.
K_x
RADIANS/KM

FIGURE 5

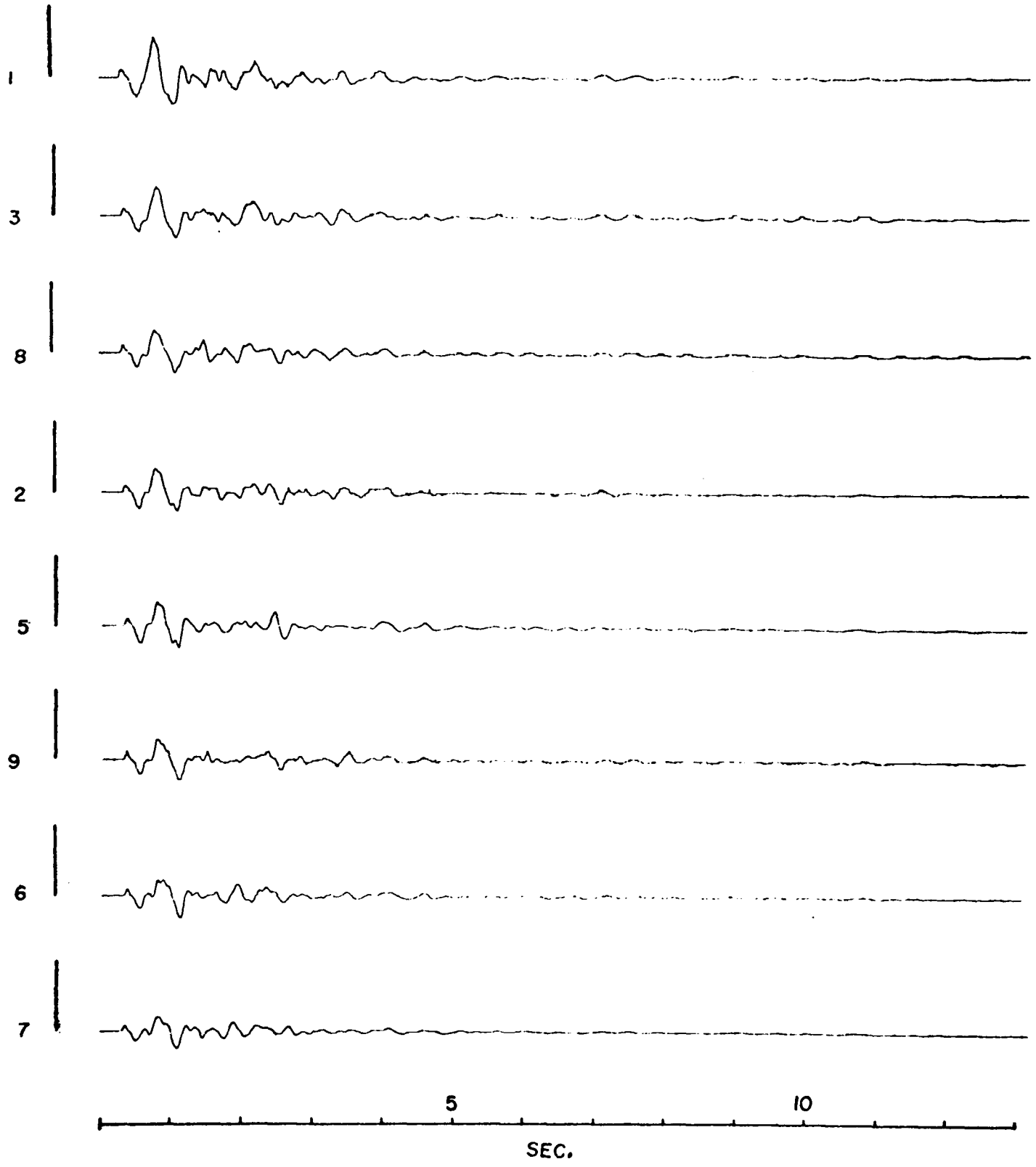

LIPTAUER VERTICAL

FIGURE 6

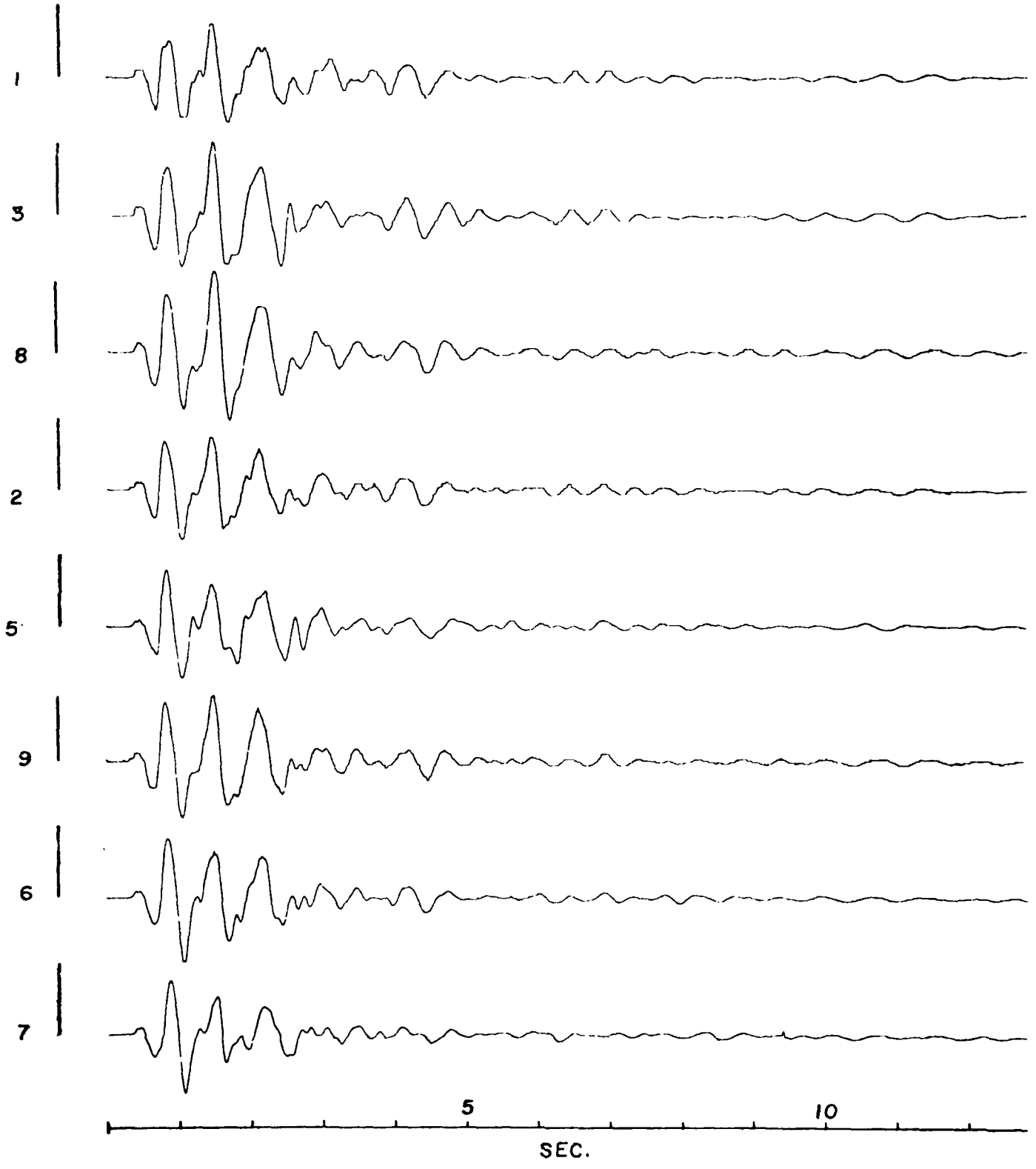

LIPTAUER RADIAL

FIGURE 7

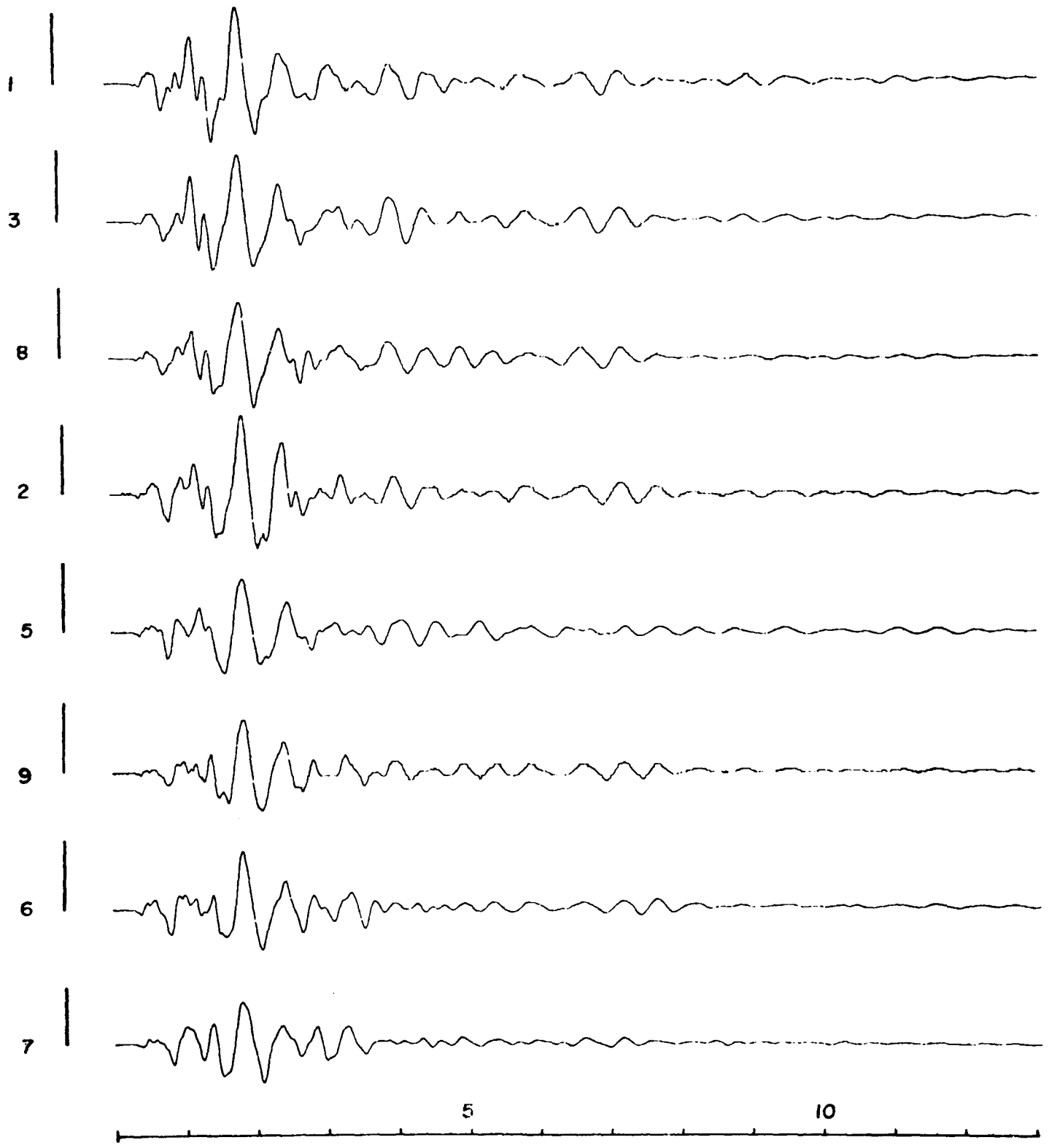

LIPTAUER TRANSVERSE

FIGURE 8

COLWICK VERTICALS

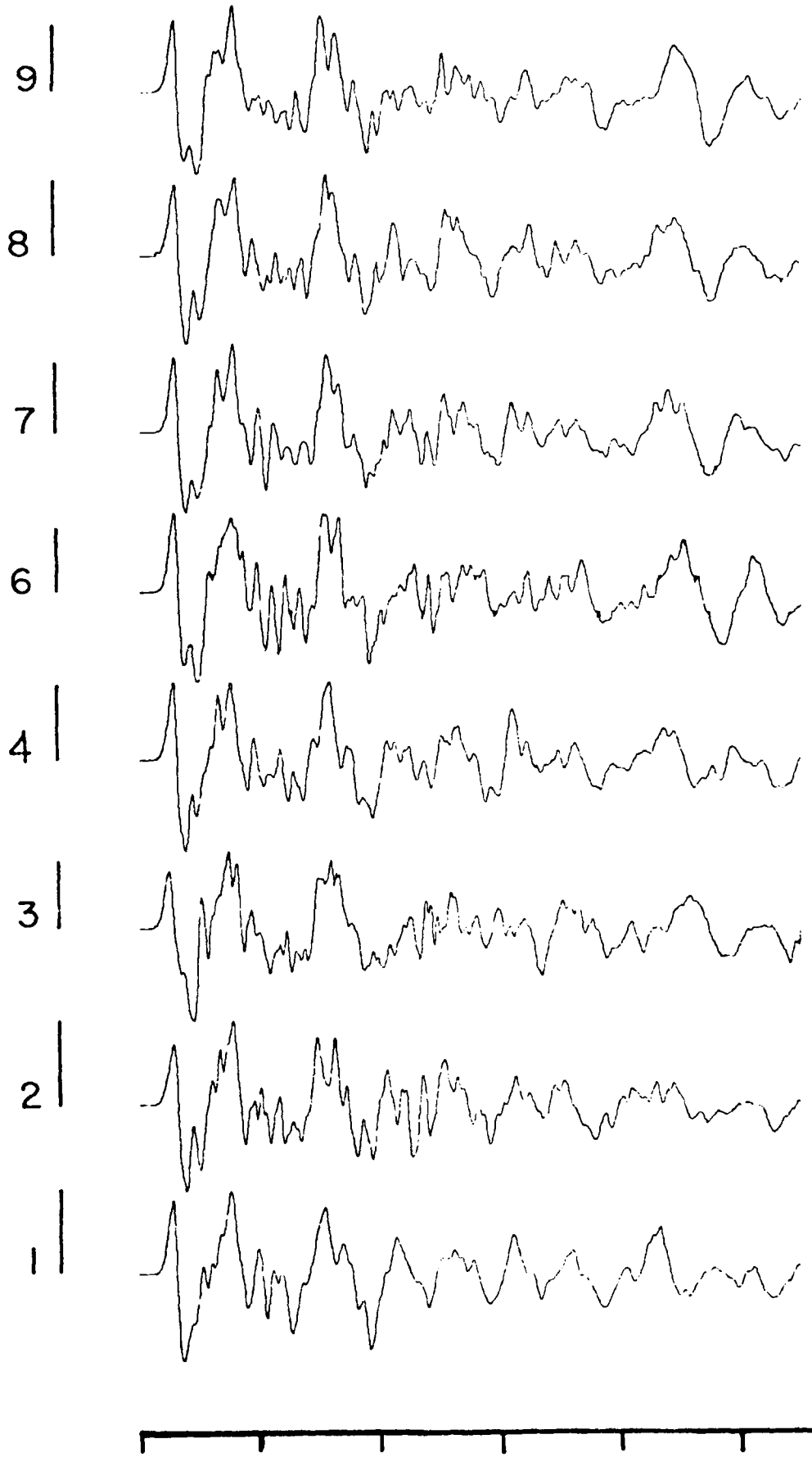

FIGURE 9

COLWICK RADIALS

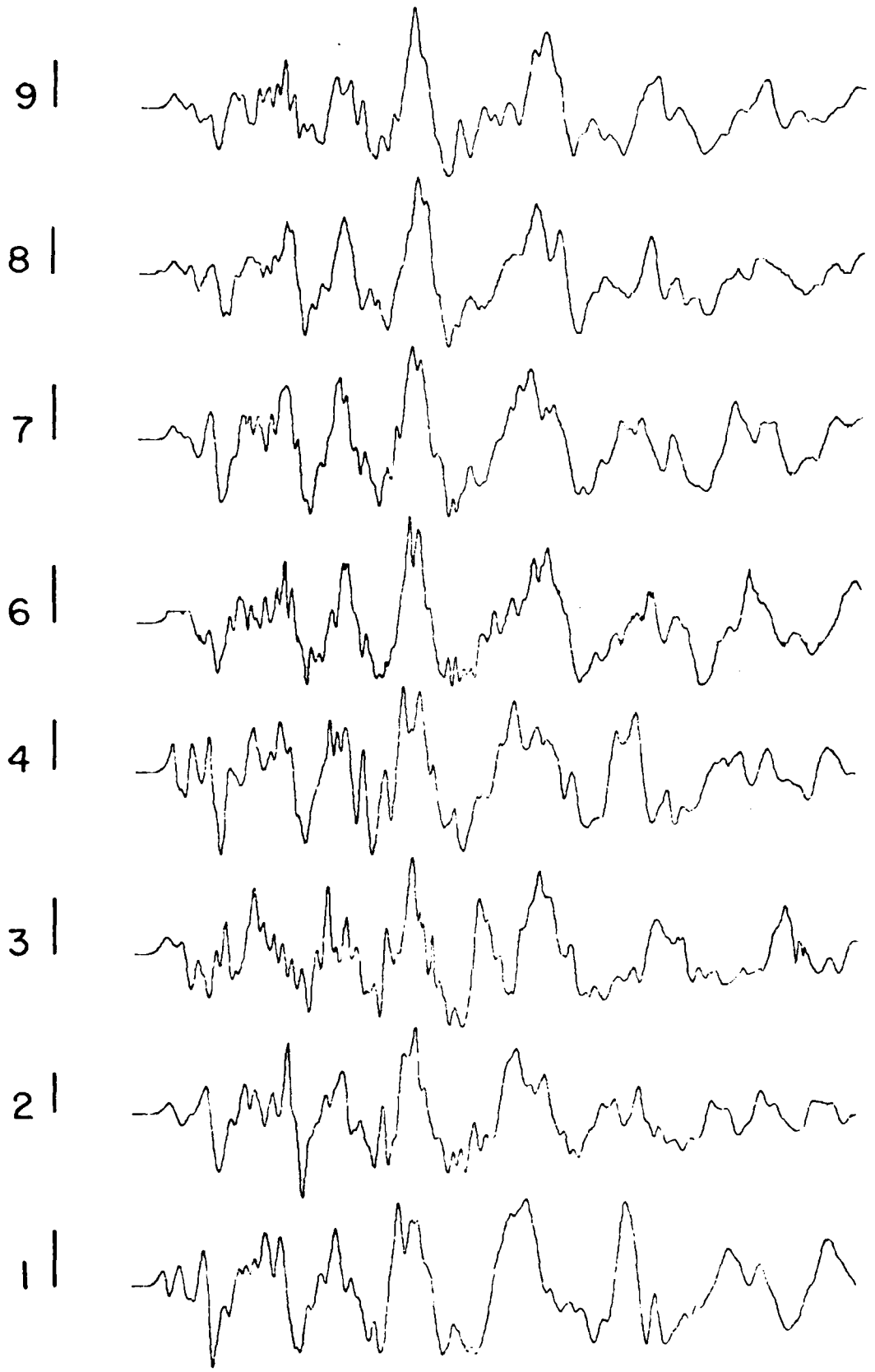

FIGURE 1

COLWICK TRANSVERSE

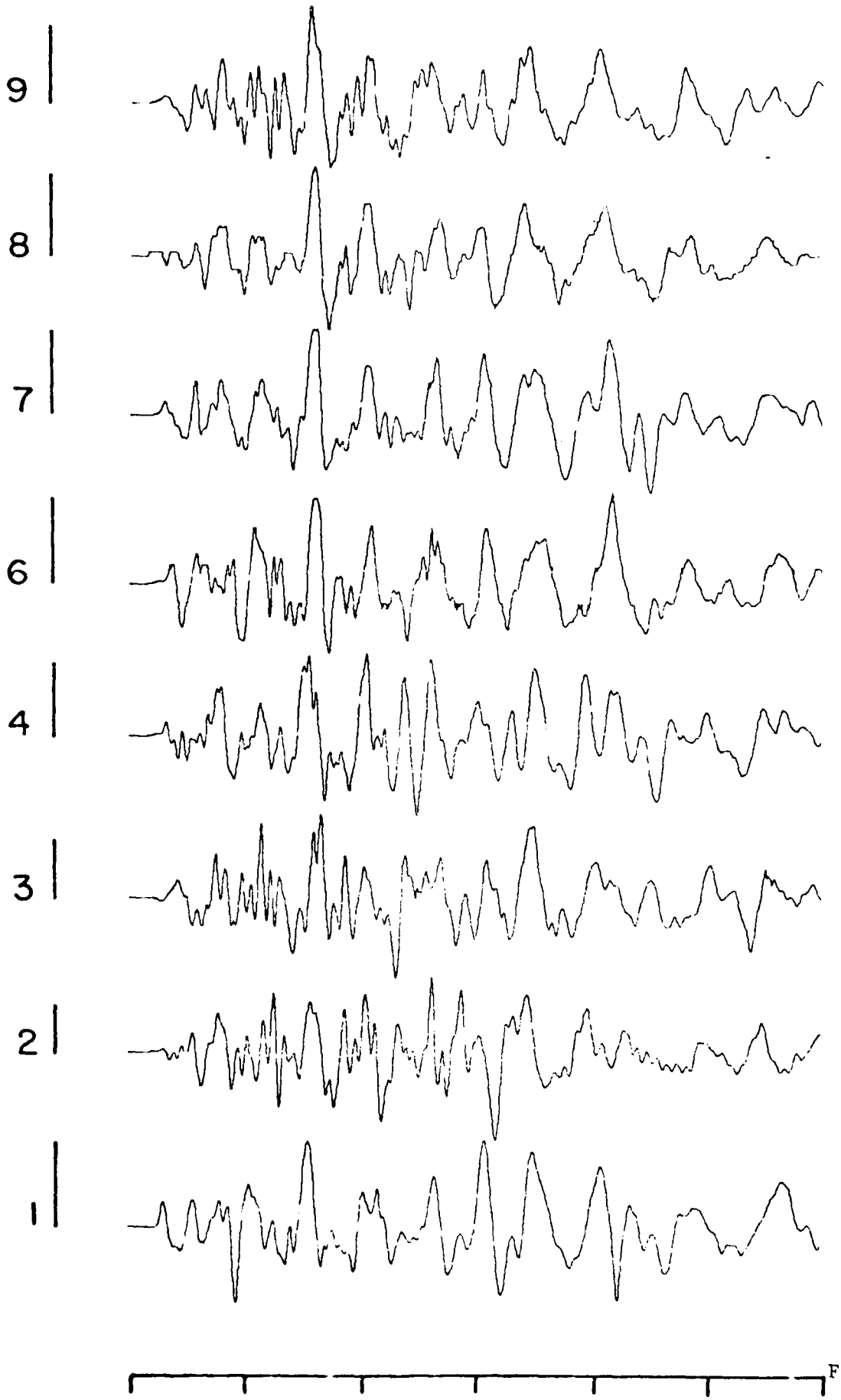

FIGURE 11

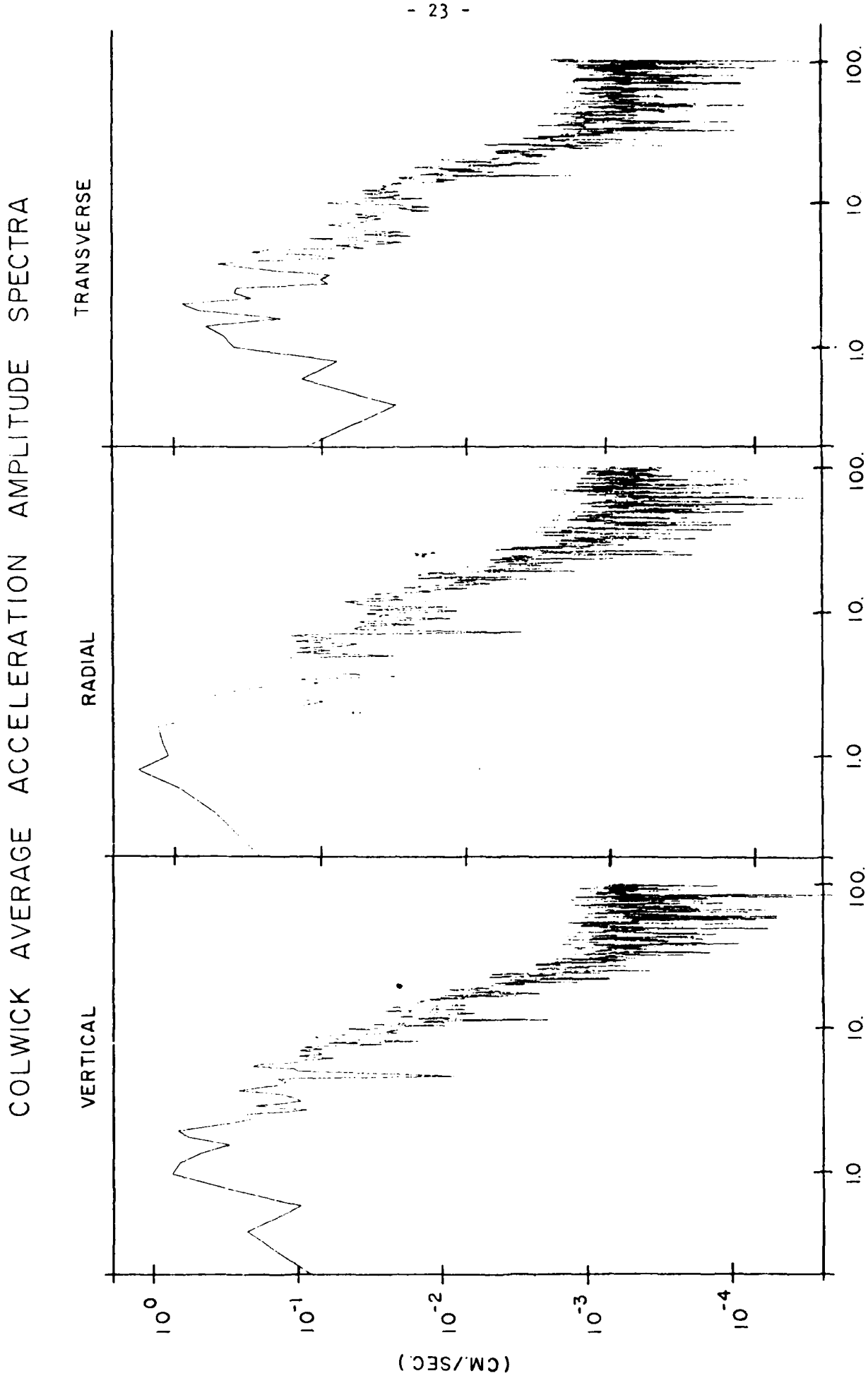
COLWICK AVERAGE ACCELERATION AMPLITUDE SPECTRA
VERTICAL
RADIAL
TRANSVERSE
(CM/SEC²)
10^{0}
10^{-1}
10^{-2}
10^{-3}
10^{-4}
1.0
10.
100.
(HERTZ)

FIGURE 12

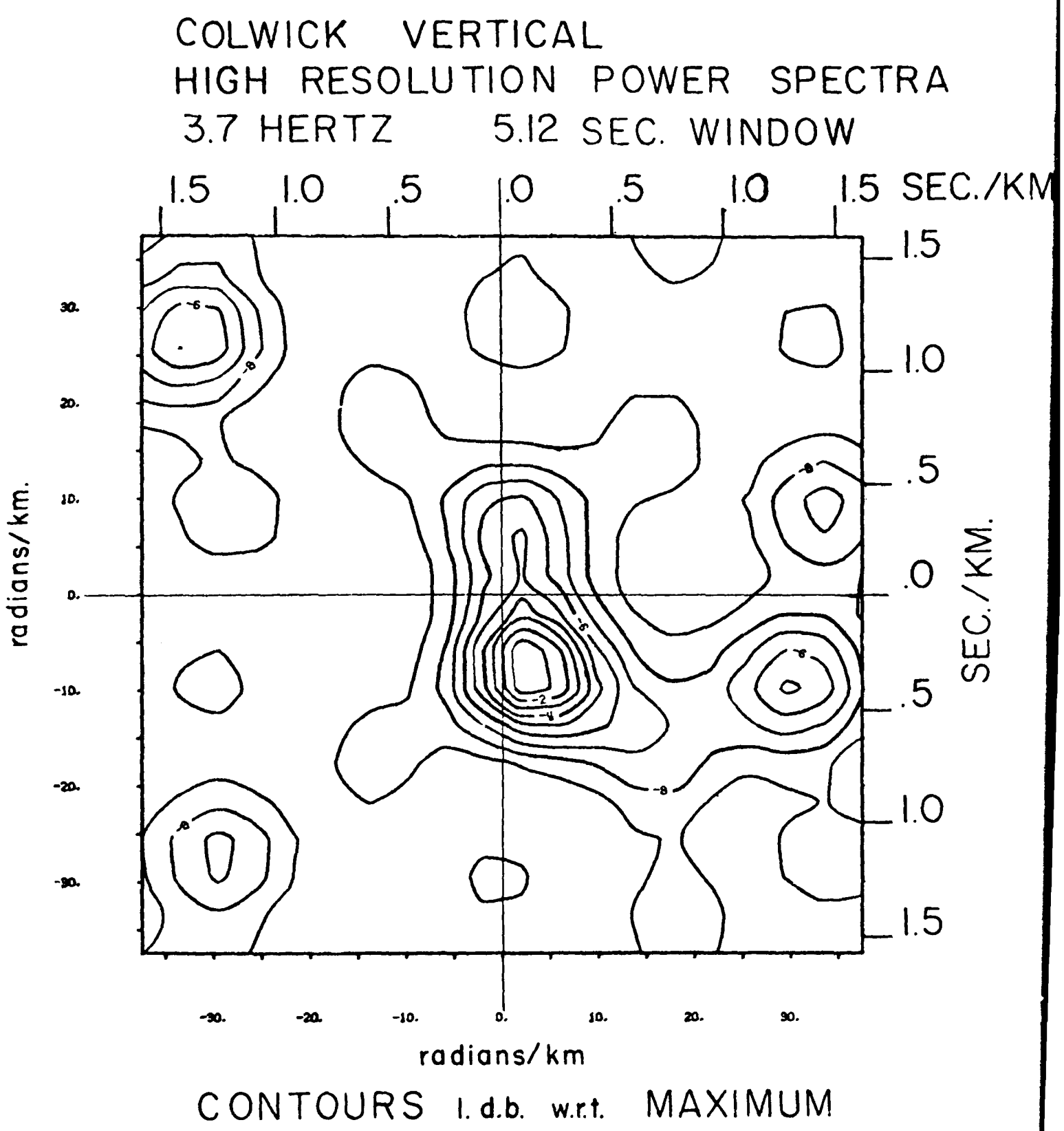
COLWICK VERTICAL
HIGH RESOLUTION POWER SPECTRA
3.7 HERTZ 5.12 SEC. WINDOW
1.5 1.0 .5 .0 .5 1.0 1.5 SEC./KM
radians/km.
SEC./KM.
30.
20.
10.
0.
-10.
-20.
-30.
radians/km
CONTOURS 1. d.b. w.r.t. MAXIMUM

FIGURE 13

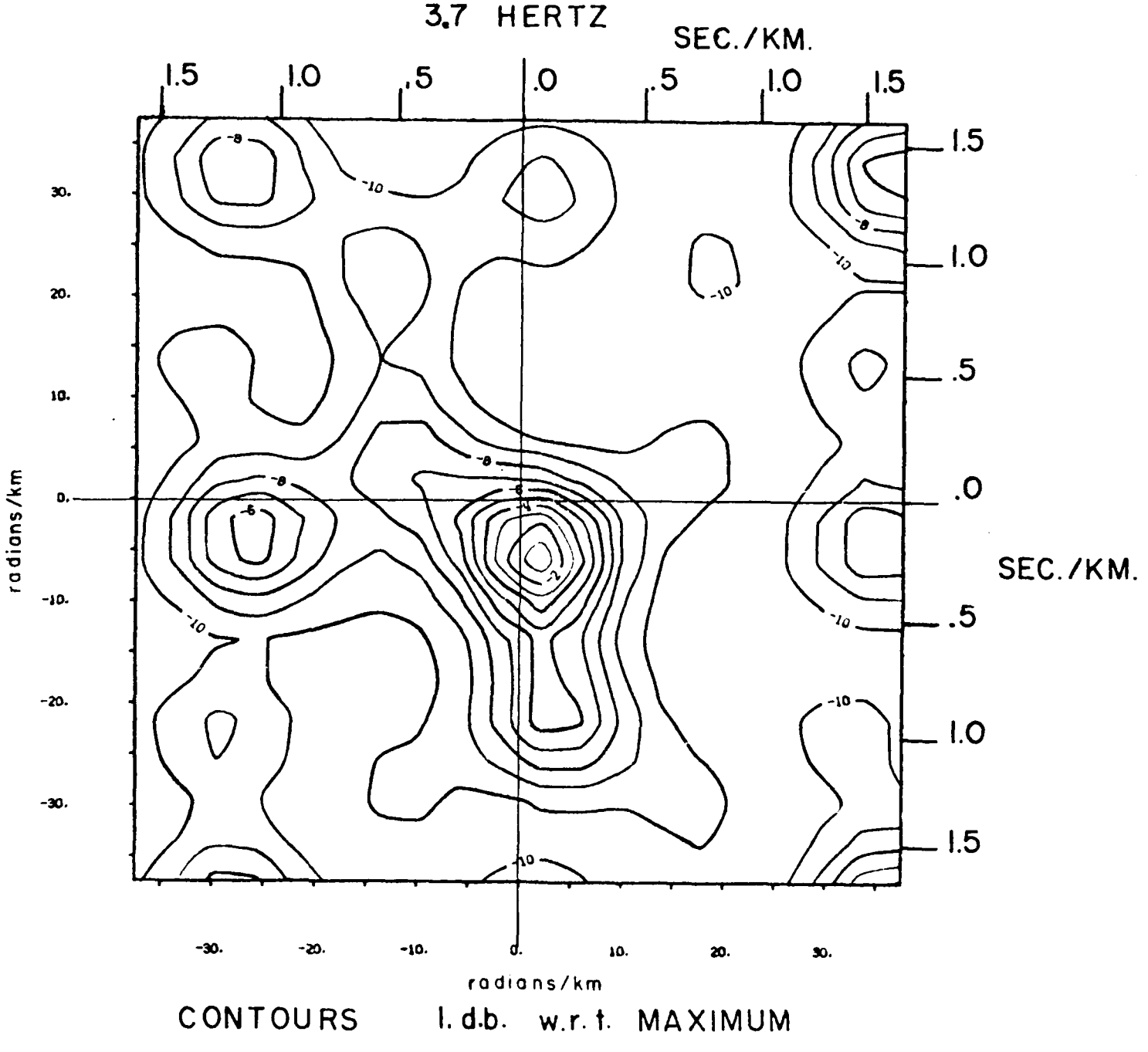
COLWICK TRANSVERSE
HIGH RESOLUTION POWER SPECTRA
3.7 HERTZ
SEC./KM.
1.5
1.0
.5
.0
.5
1.0
1.5
30.
20.
10.
0.
-10.
-20.
-30.
radians/km
-30.
-20.
-10.
0.
10.
20.
30.
radians/km
SEC./KM.
CONTOURS 1. d.b. w.r.t. MAXIMUM

FIGURE 14

COLWICK VERTICAL COMPONENT TWO STATION CROSS-CORRELATION 5.12 SEC. WINDOW

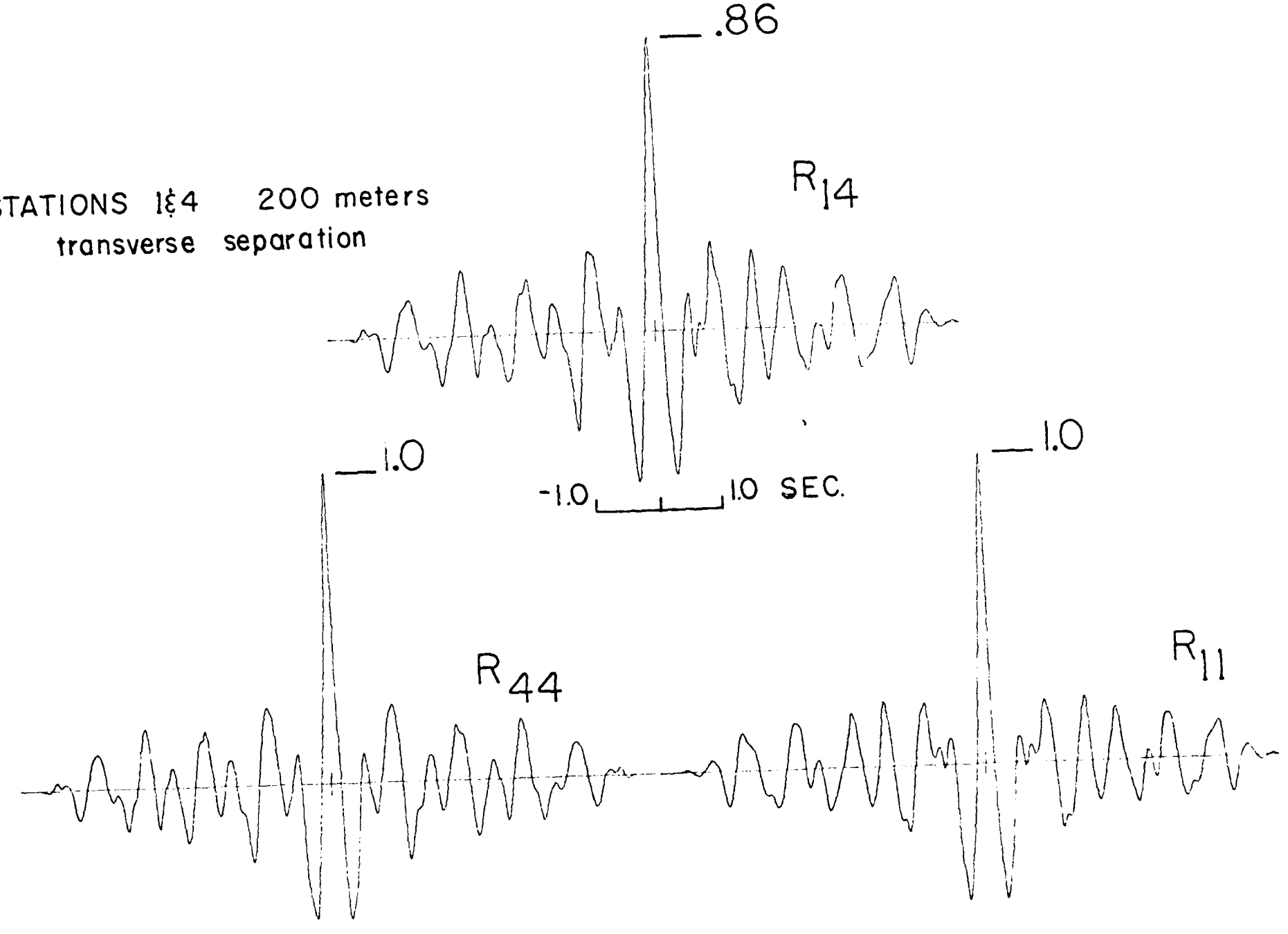

SPATIAL DECAY OF TWO STATION CROSS-CORRELATIONS

5.12 SEC. WINDOW

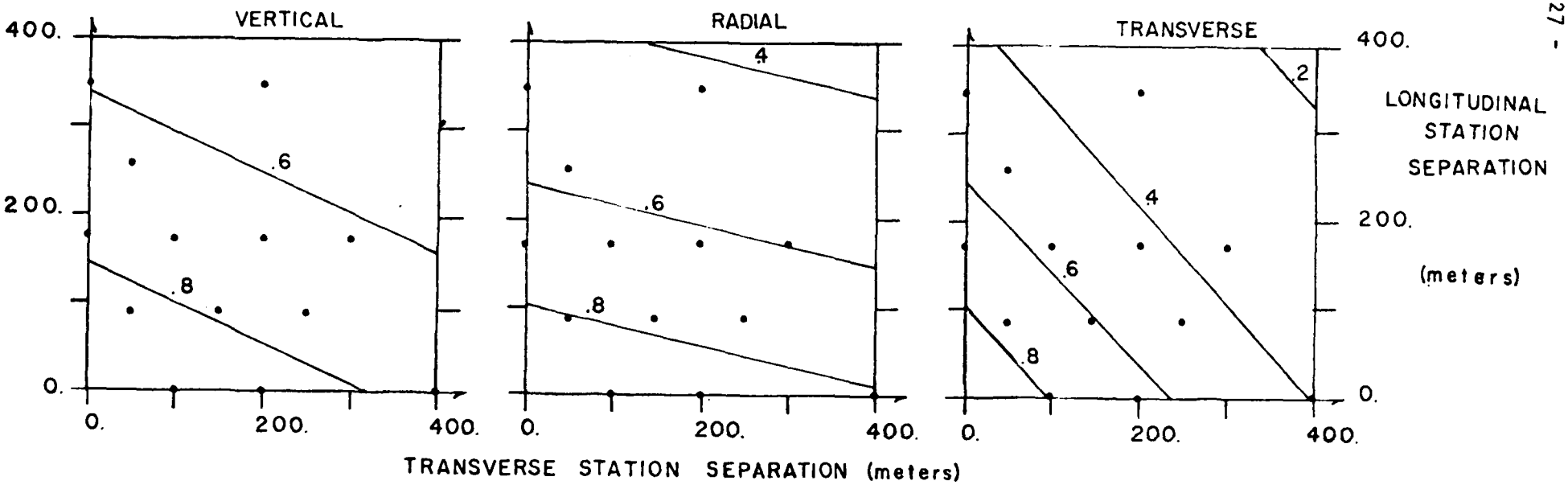

FIGURE 16

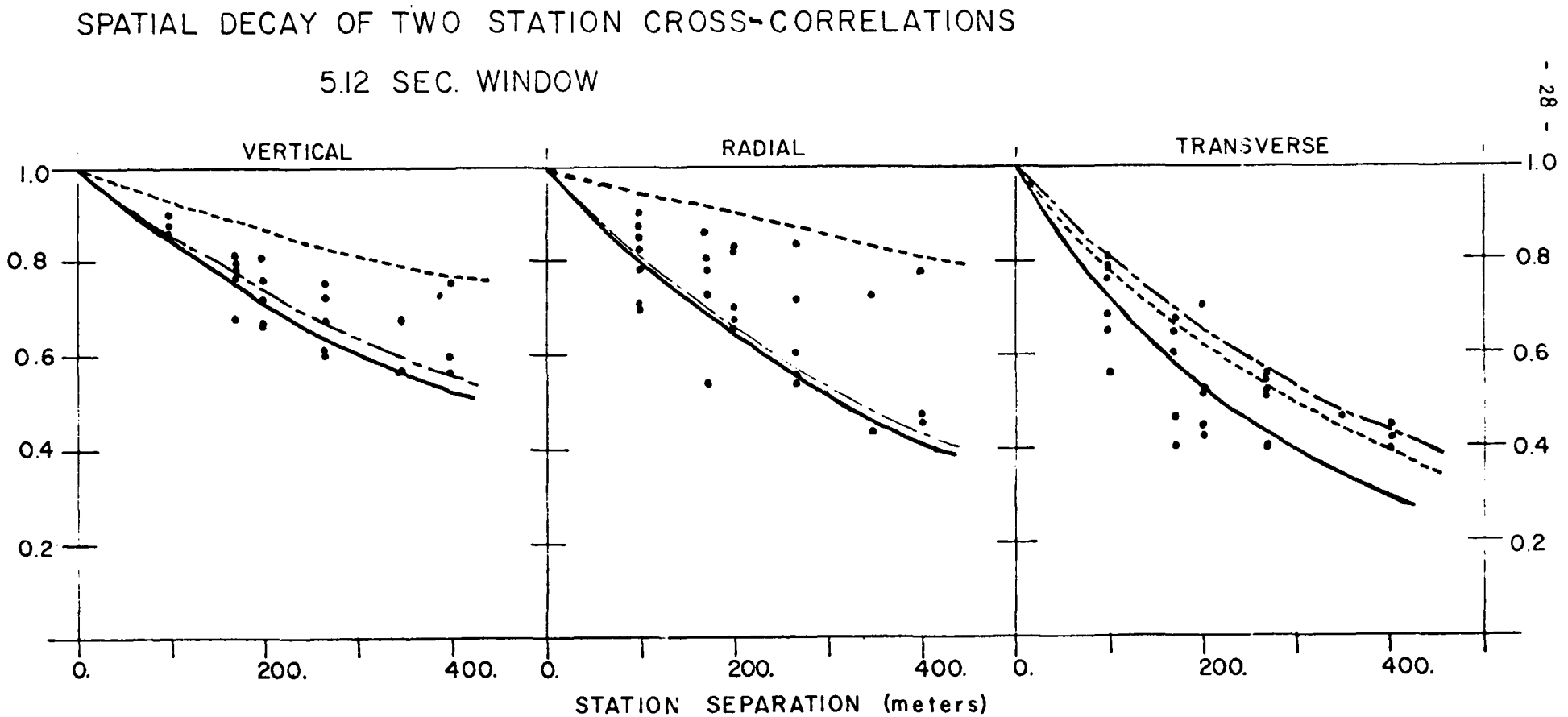
SPATIAL DECAY OF TWO STATION CROSS-CORRELATIONS
5.12 SEC. WINDOW
VERTICAL
RADIAL
TRANSVERSE
1.0
0.8
0.6
0.4
0.2
0.
200.
400.
STATION SEPARATION (meters)

FIGURE 17

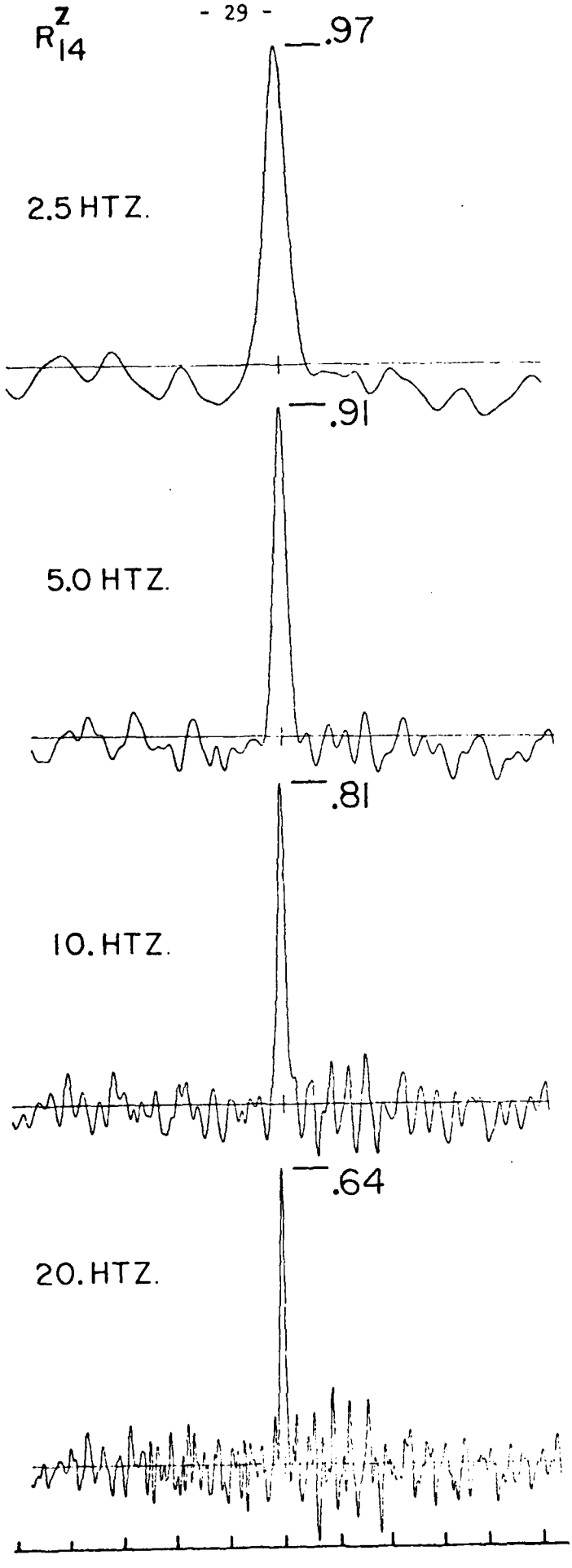

FIGURE 18

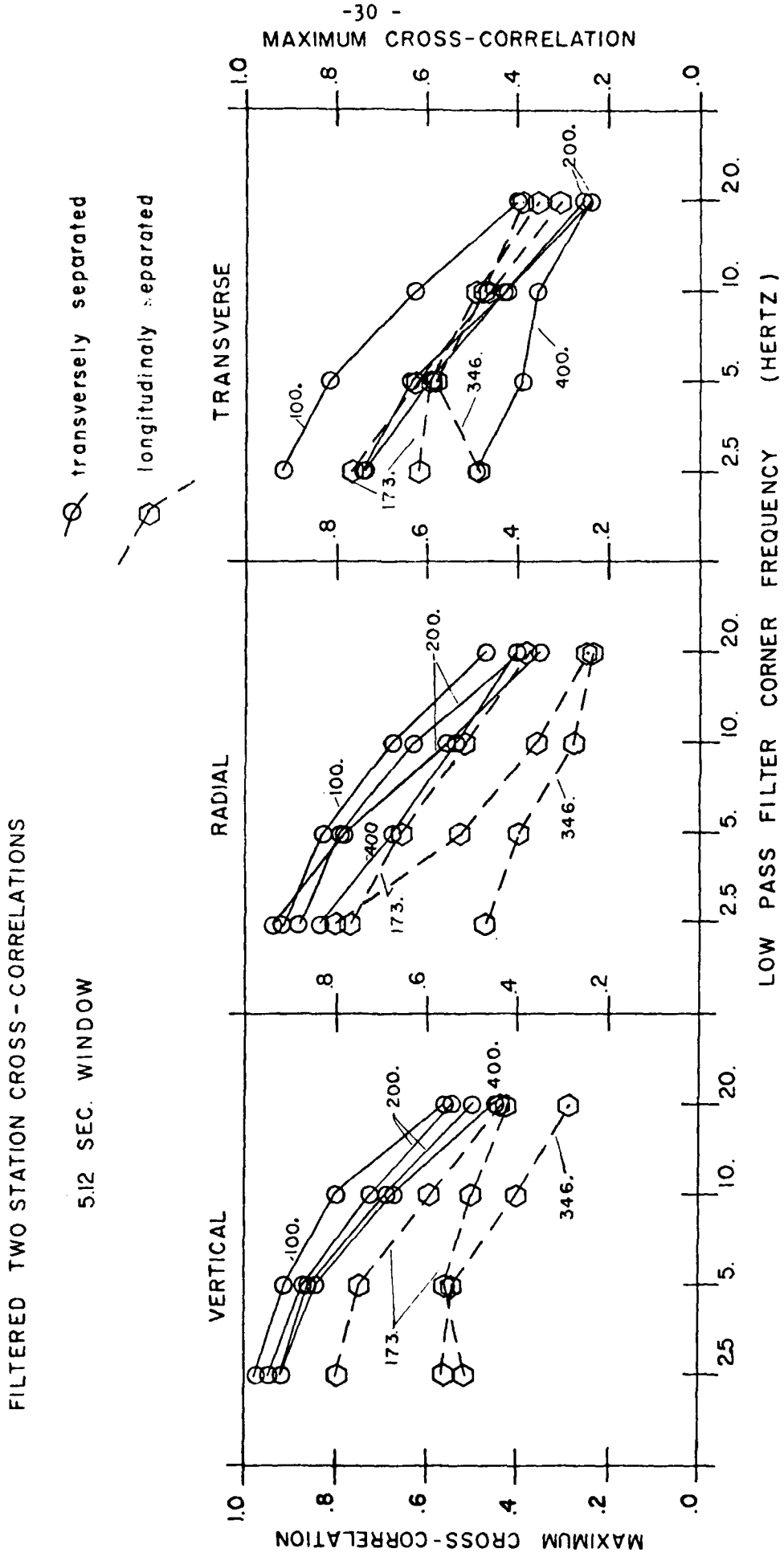
FILTERED TWO STATION CROSS-CORRELATIONS
5.12 SEC. WINDOW
transversely separated
longitudinaly separated
MAXIMUM CROSS-CORRELATION
MAXIMUM CROSS-CORRELATION
TRANSVERSE
RADIAL
VERTICAL
LOW PASS FILTER CORNER FREQUENCY (HERTZ)
100.
173.
200.
346.
400.

FIGURE 19

III. REGIONAL CRUSTAL MODEL FROM SURFACE WAVES

In previous reports, we discussed the proposed seismic studies using seismograms recorded at regional distances (0 - 10°), summarizing the type of surface wave data available for analysis, the planned method of computing observed dispersion and attenuation data, and a specific planned crustal investigation at the Nevada Test Site (NTS).

Through a substantial effort in the past year, we have succeeded in the development of methods to analyze and interpret a large body of regional broadband surface wave data generated by nuclear explosions and collapses at NTS. Following Herrin and Goforth (1977), we developed a Phase-Matched Filter (PMF) Program and other computer routines to be used in the problem of obtaining Q and velocity structure from observed group velocity, phase velocity, and attenuation coefficients of fundamental and higher mode surface waves.

Numerical tests show that PMF is superior to filtering techniques such as Moving Window Analysis (MWA) of Landisman, Dziewonski and Sato (1969). In MWA, modal interference and large secondary arrivals often cause observed dispersion curves to be discontinuous. In PMF, however, we take advantage of the approximately known regional dispersion characteristics to construct a filter which we apply to digitized surface wave data. As a result, the signal dispersion is removed. In the time domain, it corresponds to the compression of signal energy to a short symmetrical pulse. Random noise and multipathing energies are removed by appropriate windowing centered at the pulse maximum. Iterative application to seismograms recorded at several sites yields both group velocity and attenuation properties of the uncontaminated waveform.

Figures 1 and 2 show a typical result. Shown are the seismogram and two sets of observed Rayleigh wave dispersion data obtained by applying PMF and MWA, respectively, to the broadband data recorded by the seismic network of the Lawrence Livermore National Laboratory. The filter used in the PMF has been constructed from a modified velocity model of the Great Basin by Priestly and Brune (1978). We found that MWA failed to yield useful dispersion data outside the period range 7-30 seconds. Application of PMF to digitized surface wave data generated by large events (mag $\geq$ 5.5) in the distance range of 2-4° usually produce excellent dispersion and amplitude data in the period range 5-50 seconds, which represent a substantial broadening of the data bandwidth. Confidence in the extended data came from the fact that results for a given station are consistent from event to event, but different from values at other stations and from the starting model (represented by the input group velocity curve).

Figures 3 and 4 show the partial derivatives of Rayleigh wave phase velocity and the surface wave Qr with respect to shear velocity for the slightly dissiptative continental crustal model of Table 1. The result illustrate that amplitude data can play a significant role in surface wave inversion because they are strongly dependent on the velocity structure, and also that the high sensitivity of the phase velocity and amplitude of the first higher mode to the crustal shear wave velocity offers a means to improve depth resolution. Emphasis is now on experimental tests to find an approximate strategy for inversion and starting model selection for the NTS data set.

References:

Herrin, Eugene and Tom Goforth, 1977, Phase-matched filters: Application to the study of Rayleigh waves, Bull. Seis. Soc. Am., Vol. 67, No. 5, pp. 1259-1275.

Landisman, M., A. Dziewonski and Y. Sato, 1969, Recent improvements in the analysis of surface wave observations, Geophys. J., 17, 369-402.

Priestley, K. and J. Brune, 1978, Surface waves and the structure of the Great Basin of Nevada and western Utah, J. Geophys. Res., 83, 2265.

TABLE 1

Depth km	V_p km/sec	V_s km/sec	Q_p	Q_s	Density gm/cc
0.0	5.20	3.30	600	300	2.60
6.0	6.40	3.90	1000	500	3.00
36.0	8.00	4.62	1600	800	3.35

Crustal model used for data shown in Figures 3 and 4.

POOL. MAR. 17 1976 Z-Comp
recorded at ELKO Δ=397.6 KM

20 SECONDS

3.56 KM/SEC

FIGURE 1

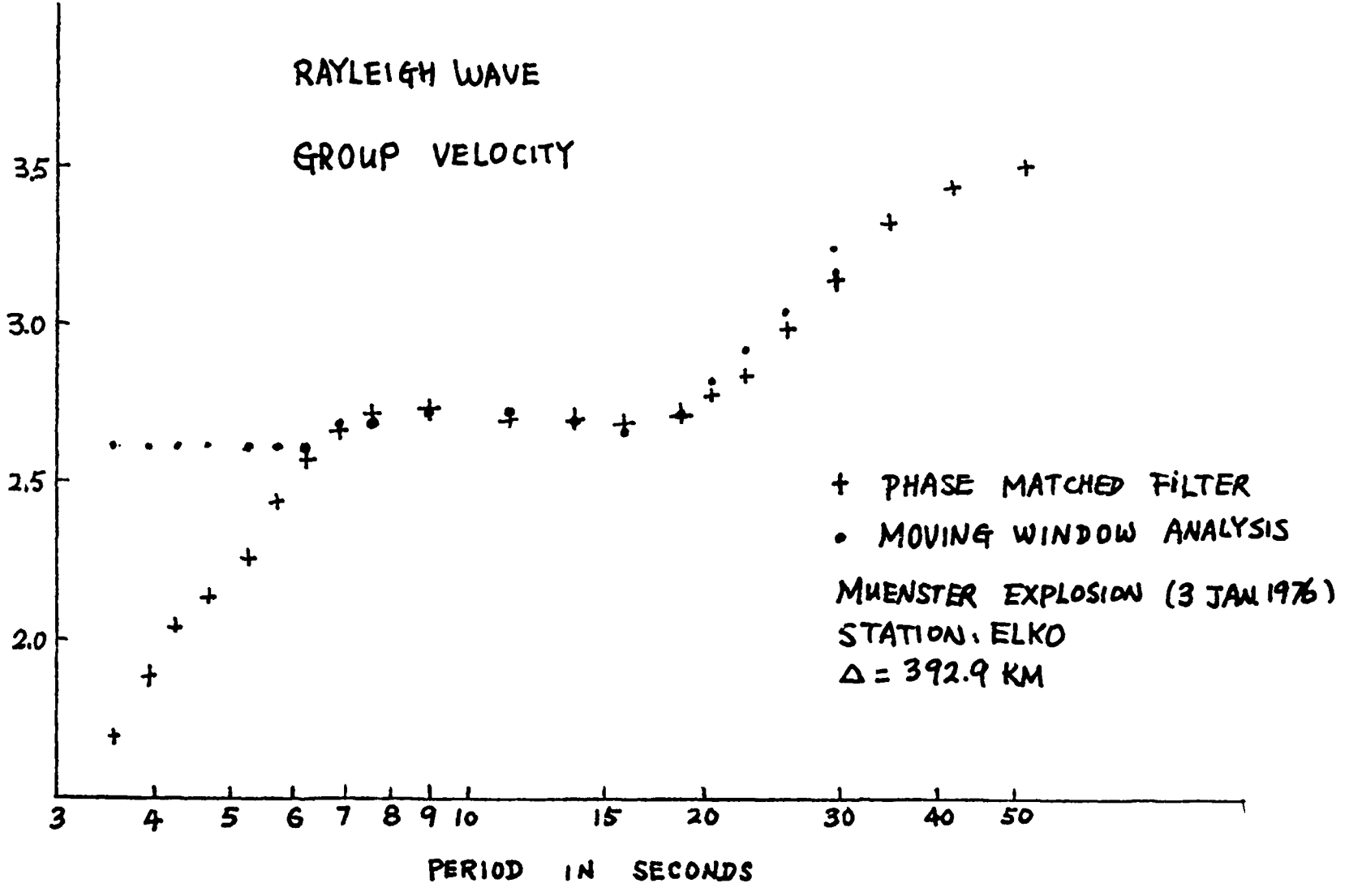

FIG. 2 COMPARISON OF GROUP VELOCITIES COMPUTED BY TWO DIFFERENT METHODS

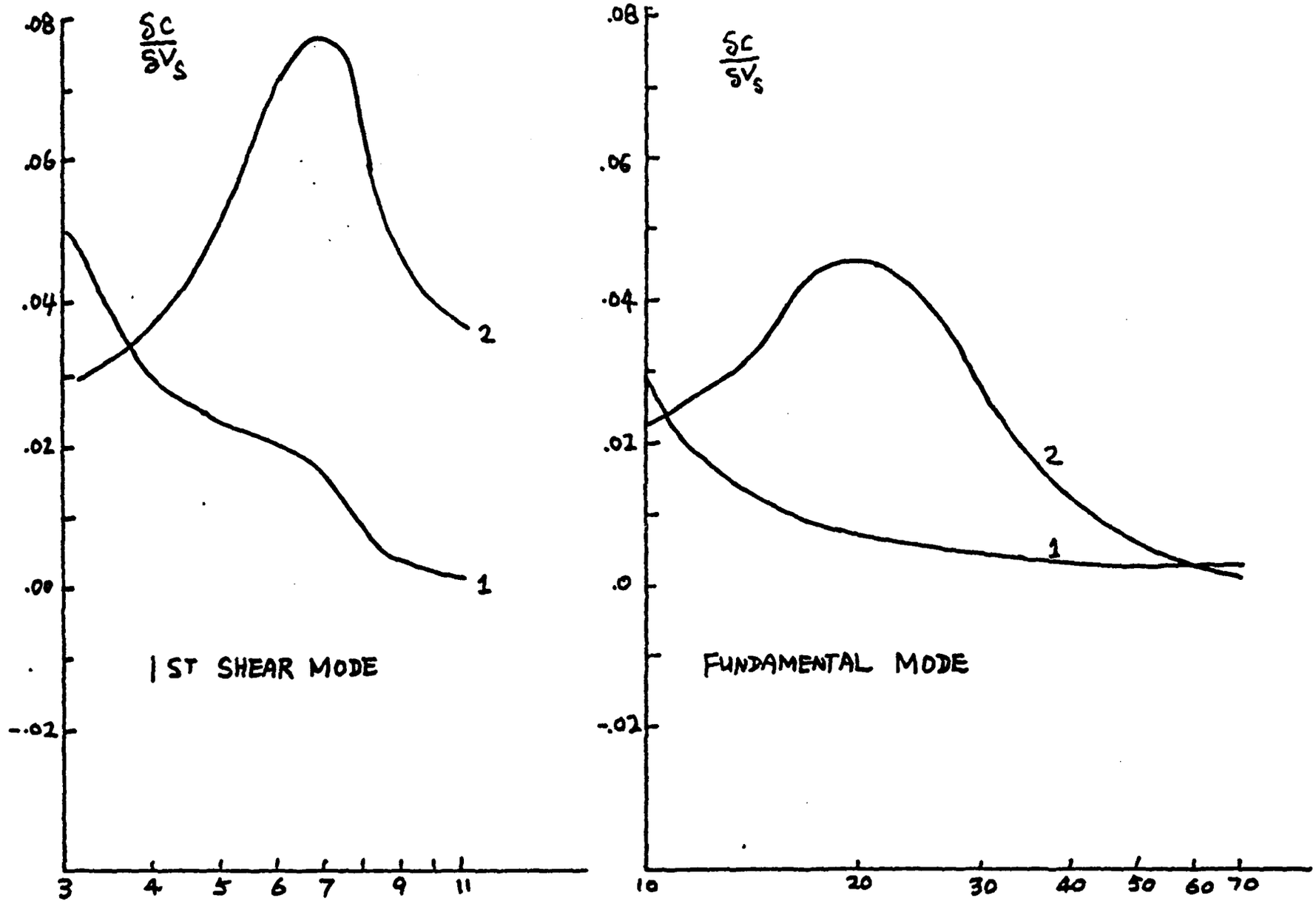

FIG. 3 The derivatives $\delta c/\delta V_s$ for the crustal model shown in table 1. Layers are indicated.

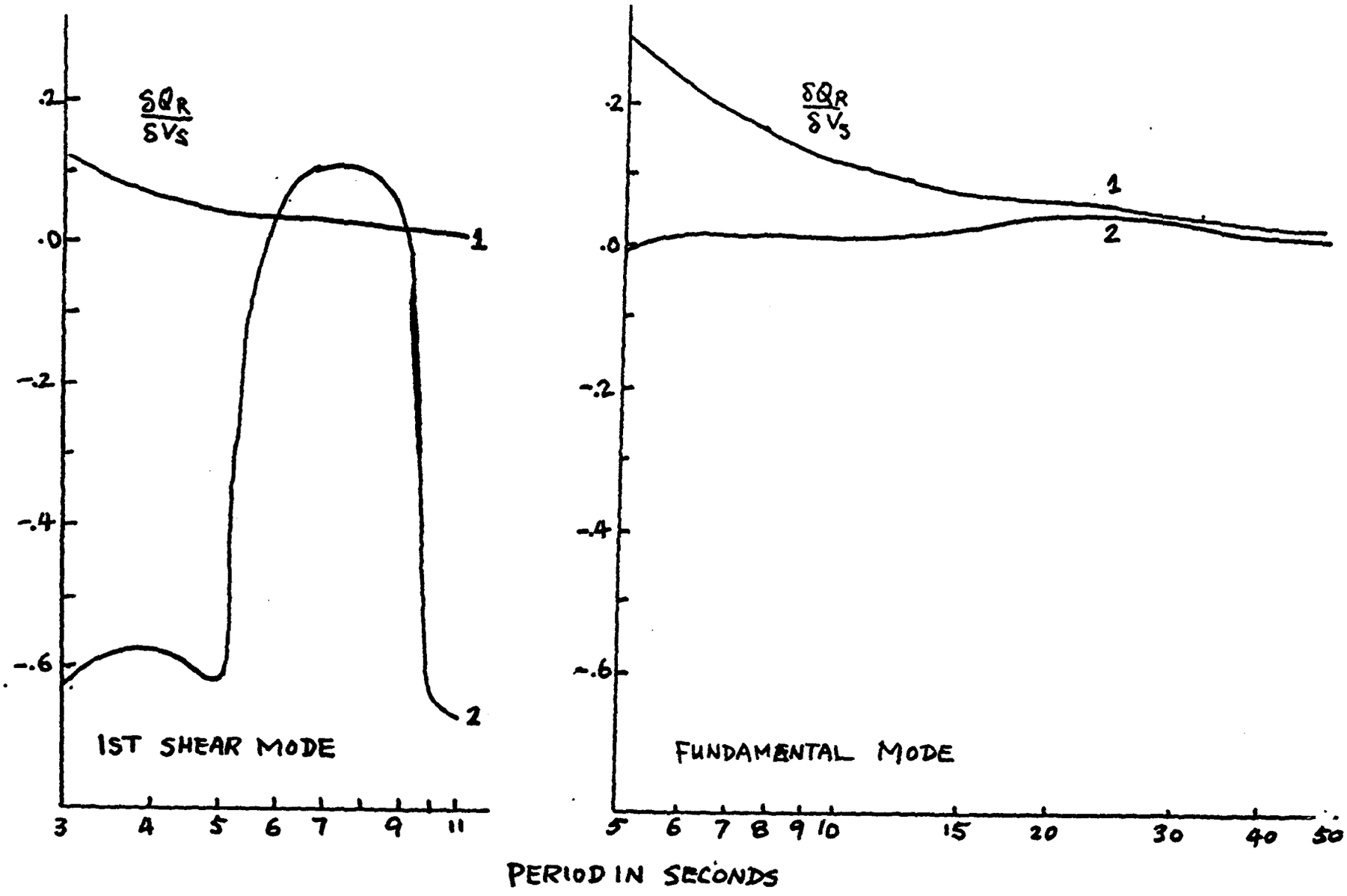

FIG. 4 The derivatives $\frac{\delta Q_R}{\delta V_S}$ for the Crustal model Layers are indicated.

IV. NEAR-SOURCE EFFECTS ON P WAVES

(A review submitted in response to a DARPA request in February 1980)

The matter of the generation of elastic waves by an explosion buried in the earth would appear to be a relatively simple problem. Thus the exercise of characterizing an explosion through the analysis of the radiated elastic waves should be quite tractable and yield definitive results. In practice, this has not proved to be a simple process, and there remain several unanswered questions concerning the relationship between an explosive source and the waves that are emitted from the source region.

Part of the difficulty undoubtedly relates to the fact that observed seismic waves contain the combined effects of the source and the propagation between source and receiver, and it is often difficult to separate these two effects. However, with current knowledge about earth structure and the improving capability for calculating the propagation effects, only a diminishing amount of the difficulty can be attributed to this cause. In what follows, therefore, it will be assumed that propagation effects outside the immediate source region can be calculated and are not a major obstacle in the interpretation. However, it is important to keep in mind this basic fact that the effects of source and propagation are often indistinguishable, and unless one is known the other can not be uniquely determined.

Setting aside the effects of propagation outside the source region, we must consider the possibilities that the waves generated by an explosion are not as simple as we might expect or that the waves are modified by effects very near the source. In most cases it is not very

meaningful to try to separate these two possibilities, and so it is useful to combine them and consider the waves that propagate outward from a general source region, which is taken to be a region surrounding the explosion and including part of the crust in the immediate vicinity.

The subject of this summary will be our current understanding of these waves that propagate outward from the source region of a buried explosion. The discussion will be mainly restricted to the P waves, and thus only body waves will be considered.

Theoretical Considerations. The problem which has the most physical similarity to that of a buried explosion and also has an analytic closed-form solution is that of a pressure pulse applied to the interior of a spherical cavity in a homogeneous elastic medium. Although many differences remain between this idealized mathematical problem and the actual situation of an explosion in the earth, it is reasonable to expect that its solution might provide a first approximation to the more complicated problem.

The solution to the problem of a pressure pulse in a spherical cavity is well-known, and numerous treatements can be found in the literature (for example: Jeffreys, 1931; Sharpe, 1942; Blake, 1952; Favreau, 1969). Because of the spherical symmetry of the problem, the solution can be expressed in terms of a scalar function known as the reduced displacement potential, which is only a function of the reduced travel time. The usual procedure is to specify the pressure history within the cavity, solve for the reduced displacement potential, and then obtain the displacement at any point by taking the gradient of

the reduced displacement potential divided by the distance from the source.

Because of its simple form, the reduced displacement potential has become a popular device for characterizing an explosive source. Since it is independent of distance, it can be determined at any convenient distance from the source. This is helpful in dealing with the complications of an inelatic zone which surrounds large explosions. The initial cavity of a contained explosion will in general be surrounded by successive zones of vaporization, melting, cracking, and inelastic stresses before reaching a zone where the assumptions of linear elasticity are appropriate. In place of the radius of the initial cavity, it is customary to use the inner boundary of the region of elastic behavior as the effective source radius. This is often called the elastic radius. With this modification of the problem the pressure history within the cavity gets replaced by the stress wave which arrives at the elastic radius.

It should be noted in passing that the problem where the source consists of shear stresses applied to the interior of a spherical cavity also has known solutions (Jeffreys, 1931; Honda, 1960). However, so far these results seem to have found little application in the problem of a buried explosion.

A spherically symmetric source, such as a pressure pulse in a spherical cavity, generates only P waves. However, if such a source is placed in a medium with a preexisting shear stress, then S waves will also be generated (Archambeau, 1972). Closely related to this mechanism

is that of triggering a tectonic earthquake on a nearby fault (Andrews, 1973). In either case the secondary source related to the shear stress has the form of a shear dislocation, and so its radiation pattern is a quadrapole and it is roughly an order of magnitude more efficient in generating S waves than P waves. Thus, observational studies of this effect have been based primarily on S waves and surface waves (Press and Archambeau, 1962; Aki et al., 1969; Archambeau and Sammis, 1970; Toksoz et al., 1971; Lambert et al., 1972; Aki and Tsai, 1972; Toksoz and Kehrer, 1972). It appears from the results of these studies that, while reasonable levels of prestress can be important in the generation of S waves and surface waves, the direct P waves generated by this secondary source will be small compared to those generated by the explosive source. However, the mechanism whereby S waves from the secondary source are converted to P waves at nearby boundaries could be an important source of P waves.

The next step in constructing a more realistic model for a buried explosion in the earth is to consider the effects of material inhomogeneity in the vicinity of the explosion. Such inhomogeneity causes the reflection and refraction of primary waves from the source, the conversion of wave type from P to S and vice versa, and the generation of interface waves. For shallow explosions, a very important inhomogeneity is the free surface of the earth. Geologic layering, the water table, and fault surfaces are other types of inhomogeneities which can also have significant effects.

Attempts to obtain exact solutions to the problem of an explosion in the vicinity of an inhomogeneity have not been very successful.

The problem of a finite spherical source embedded in a homogeneous elastic halfspace has been considered by Ben-Menahem and Cisternas (1963) and by Thiruvenkatachar and Viswanathan (1965, 1967). This is a problem with mixed boundaries and its solution is very difficult, the answer usually being expressed as an infinite series. Because of the rather untractable form of the results, the analytical treatment of this problem has not yet contributed any practical results to the problem of a buried explosion.

Provided one is willing to approximate an explosion with a point source, the effect of vertical inhomogeneity in the vicinity of the source can be handled in a satisfactory manner. Two approaches are commmonly used, the method of generalized rays (Helmberger and Harkrider, 1972) or the method using propagator matrices (Fuchs, 1966; Hasegawa, 1971).

The treatment of lateral inhomogeneity near an explosive source is a more difficult problem. This would include such features as dipping layers, faults, and surface topography. In general, numerical methods are required to calculate the effects of this type of inhomogeneity, but usually the detailed knowledge about the geometry of such features is not sufficient to justify an elaborate computational treatment.

The presence of inhomogeneity near the explosive source can also lead to additional inelastic effects. Spallation is an important effect of this type. When the P wave from an explosion is reflected at the free surface with a change in sign, the associated stress can cause failure in tension of the near surface material. When failure occurs,

part of the near-surface material may separate and move ballistically upward, eventually falling back and impacting the earth at some later time. This closure of the spall is sometimes referred to as slapdown. This process of spallation has been fully described and documented in the literature (Eisler and Chilton, 1964; Eisler et al., 1966; Chilton et al., 1966; Perret, 1972; Viecelli, 1973; Springer, 1974). The energy in the P wave which leaves the source in an upward direction is converted into a reflected pP wave, a reflected sP wave, a surface wave, inelastic effects, and the waves generated by the slapdown. Viewed from a distance, the primary effects of spallation upon the P-wave coda is a diminished amplitude of the pP wave and an additional phase at the time of slapdown.

On the basis of the preceding discussion, it is possible to construct a general model of a buried explosion. The model is primarily an elastic model so it begins with a stress pulse applied at the elastic radius. This generates an outward propagating P wave and, if the source region is prestressed, also an S wave. These outward propagating waves interact with inhomogeneities in material properties near the source to produce reflected and interface waves. Waves reflected from above the source may also cause spallation and the associated slapdown. The outward propagating waves may also trigger secondary shear dislocations at near-by stress concentrations. All of these effects combine and interact to produce the waves that propagate out from the general source region.

Experimental Results. Consider now the question of what can be learned about a buried explosion from an analysis of experimental data. This is a basic inverse problem. The effects, primarily the waveforms of elastic waves, are to be used to estimate properties of the cause, the explosive source. The usual approach is to construct a general model of the source containing a number of undetermined parameters. The observational data are then analyzed to deterimine whether the model is capable of explaining the data and, if so, what values should be given to the parameters.

Because of the advantages already mentioned, it has become common to characterize an explosive source by its reduced displacement potential, and so the experimental determination of the reduced displacement potential has received considerable attention. The generalized form of the reduced displacement potential as a function of time is an abrupt start, a smooth rise to a maximum over a finite time, and then a decrease to a static level. Three numbers - the rise time, the static value, and the ratio of maximum to static values - describe the major features of such a function. In the frequency domain, the first time derivative of the reduced displacement potential has a correspondingly simple form. Going from high to low frequencies, the spectrum rises at some slope, reaches a maximum near what is called the corner frequency, and then decreases to a constant value at low frequencies. In terms of the time domain parameters, the spectral amplitude scales with the static value, the frequency scales with the rise time, the ratio of the spectral maximum to the low frequency level depends upon the ratio of maximum to static values of the reduced displacement

potential, and the high frequency slope depends upon the abruptness of the beginning of the reduced displacement potential.

The simple model of a pressure pulse applied to the interior of a spherical cavity can be used to relate the parameters of the reduced displacement potential to the physical properties of the explosive source. The static value depends upon the static pressure, the cavity volume, and the material properties. The rise time depends upon the cavity radius and the material properties. The ratio of maximum to static values, sometimes called the overshoot, depends upon the time history of the pressure pulse and the material properties. Considering the pressure pulse to consist of two main parts, an impulse and a step, the overshoot will increase as the ratio of impulse to step increases.

For a more complete parameterization of the reduced displacement potential, it can be approximated with an analytic function. Haskell (1967) argued that displacement, velocity, and acceleration should all be continuous at the elastic radius and used a fourth order polynomial in time. Von Seggern and Blandford (1972) required that only the displacement be continuous and used a second order polynomial. Mueller and Murphy (1971) used the theoretical solution for a pressure pulse within a cavity and a semi-empirical expression for the shape of the pressure pulse to arrive at an analytic expression for the reduced displacement potential. The basic difference in these three models is primarily at the high frequencies, where the Haskell model falls off with a -4 slope on a log-log scale, while both the von Seggern-Blandford and Mueller-Murphy models fall off with a -2 slope. The experimental data (von Seggern and Blandford,

1972; Murphy, 1977; Burdick and Helmberger, 1979) at teleseismic, regional, and near distances mostly favor the -2 slope of the von Seggern-Blandford and Mueller-Murphy models. From an analysis of very-near data, Peppin (1976) found evidence for a slope of at least -3 at the high frequencies.

The problem of estimating the reduced displacement potential for an explosion can be approached from at least three directions. The dynamic equations for the explosion and the surrounding inelastic region can be solved numerically and the calculations carried out to the elastic radius (Holzer, 1966; Rodean, 1971). Another approach is to measure the ground motion as near the source as possible while still in the elastic region, and then calculate the reduced displacement potential on the basis of these measurements (Werth et al., 1962; Werth and Herbst, 1963). In most cases the reduced displacement potential can only be determined for times less than about 0.5 sec because the effect of the free surface and other departures from spherical symmetry begin to affect the results at later times. A third approach is to record elastic waves at near to teleseismic distances and then attempt to infer the reduced displacement potential which best explains the observations. What emerges from this approach is an apparent reduced displacement potential, because, as already discussed, the waves that emerge from the general source region can consist of considerably more than the direct P wave from the explosion. Such additional effects must be taken into account in the interpretation of the data.

Because of the abundance of easily accessible data, numerous studies have used waveform data recorded at near to teleseismic distances to

investigate the details of explosive sources. Various methods of interpretation have been employed. A few of the representative studies will be summarized below.

Molnar (1971), Kulhanek (1971), and Wyss et al. (1971) all studied the spectra of teleseismic P waves and found that the spectra were modulated. This can be explained, at least partly, by the interference of the P and pP waves. Filson and Frasier (1972) and King et al. (1972) fit theoretical models to the spectra of teleseismic P waves to estimate parameters of the reduced displacement potential.

Aki et al. (1974) studied both near and teleseismic data and found evidence for a large overshoot ratio in the reduced displacement potential. Peppin (1976) analyzed near and regional data and did not find evidence for overshoot. Murphy (1977) studied a variety of data from near to teleseismic distances and concluded that the data were consistent with the source model of Mueller and Murphy (1971).

Frasier (1972) deconvolved teleseismic P waves and found evidence of a pP phase plus a later phase, possibly due to slapdown. Bakun and Johnson (1973) applied homomorphic deconvolution to teleseismic P waves and found indications of the pP reflection and also a later phase which was consistent with an interpretation in terms of slapdown. Burdick and Helmberger (1979) used synthetic seismograms to model teleseismic P waves and found that the data could be explained by substantial overshoot in the reduced displacement potential and reflected crustal phases, but did not require a slapdown phase.

Stump and Johnson (1977) and Stump (1979) have developed a general inverse method for estimating the second-rank seismic moment tensor. The trace of this tensor is equivalent to the reduced displacement potential and the deviatoric components provide a means of expressing other effects, such as tectonic stress release.

There is obviously not total agreement among the observational studies concerning the source properties of explosions. This is partly due to the different methods of interpretation which have been employed. It is also due to a certain degree of nonuniqueness that exists in the basic problem. This is compounded by the fact that propagation effects must usually be taken into account in the interpretation of the data, and any uncertainty in earth structure can get translated into nonuniqueness in the source properties. For instance, a peaked spectrum of the P wave coda can be produced in at least three ways: overshoot of the reduced displacement potential, interference caused by reflected waves, or over-correction for the effects of attenuation in the interpretation process.

Conclusions. The available theoretical models of an explosive source embedded in a realistic crustal structure appear to be sufficiently general to explain the major features of the observational data. It is clear that considerably more than the direct P wave emerges from the general source region. Reflections from inhomogeneities near the explosion, particularly the free surface, are definitely important. The importance of spallation and slapdown upon the generation of P waves is still rather uncertain. Tectonic strain release may be important in some instances, and, when it is significant, it is probably not the direct P waves from the secondary sources but rather the S to P converted phases which contribute most to the P wave coda. The entire matter of how S waves are generated in the vicinity of an explosion is still not completely understood, and some new process, such as the acoustic fluidization suggested by Melosh (1979), may eventually provide the answer.

The methods of interpreting the observational data to infer source properties are steadily improving, and the increased use of synthetic seismograms and more complete inversion schemes should be very helpful. This progress in interpretation will require a more accurate knowledge of earth sturcture, because it is doubtful that the accuracy of inferred source properties can ever be greater than that of the earth model used in the interpretation. The anelastic properties of the earth present a current problem in this respect, because the correction for attenuation which must usually be applied in the interpretation process is still rather uncertain and this can have a major effect at the high frequencies.

Hopefully, continued improvements in the methods of interpretation and knowledge of earth structure will reduce the inherent nonuniqueness in this inverse problem.

The reduced displacement potential has become a popular means of summarizing the properties of an explosive source and has been quite useful. But is should be emphasized that in most cases this is only an apparent reduced displacement potential. The requirement for spherical symmetry holds, if at all, only for a few tenths of a second, and asymmetry in the source region is an important factor in most P wave codas. The importance of this point is the realization that the apparent reduced displacement potential for a given event may be different as viewed from different distances, different azimuths, or different types of data.

References

Aki, K., P. Reasonberg, T. DeFazio, Y-B. Tsai, Near-field and far-field seismic evidences for triggering of an earthquake by the BENHAM explosion, Bull. Seism. Soc. Am., 59, 2197-2207, 1969.

Aki, K., Y-B. Tsai, Mechanism of Love-wave excitation by explosive sources, J. Geophys. Res., 77, 1452-1475, 1972.

Aki, K., M. Bouchon, P. Reasenberg, Seismic source function for an underground nuclear explosion, Bull. Seism. Soc. Am., 64, 131-148, 1974.

Andrews, D. J., A numerical study of tectonic stress release by underground explosions, Bull. Seism. Soc. Am., 63, 1375-1391, 1973.

Archambeau, C. B., C. Sammis, Seismic radiation from explosions in prestressed media and the measurement of tectonic stress in the earth, Rev. Geophys. Space Phys., 8, 473-500, 1970.

Archambeau, C. B., The theory of stress wave radiation from explosions in prestressed media, Geophys. J. R. Astr. Soc., 29, 329-366, 1972.

Bakun, W. H., L. R. Johnson, The deconvolution of teleseismic P waves from explosions MILROW and CANNIKIN, Geophys. J. R. Astr. Soc., 34, 321-342, 1973.

Ben-Menahem, A., A. Cisternas, The dynamic response of an elastic halfspace to an explosion in a spherical cavity, J. Math. Phys., 42, 112-125, 1963.

Blake, F. G., Spherical wave propagation in solid media, J. Acoust. Soc. Am., 24, 211-215, 1952.

Burdick, L. J., D. V. Helmberger, Time functions appropriate for nuclear explosions, Bull. Seism. Soc. Am., 69, 957-973, 1979.

Chilton, F., J. D. Eisler, H. G. Heubach, Dynamics of spalling of the earth's surface caused by underground explosions, J. Geophys. Res., 71, 5911-5919, 1966.

Eisler, J. D., F. Chilton, Spalling of the earth's surface by underground nuclear explosions, J. Geophys. Res., 69, 5285-5293, 1964.

Eisler, J. D., F. Chilton, F. M. Sauer, Multiple subsurface spalling by underground nuclear explosions, J. Geophys. Res., 71, 3923-3927, 1966.

Favreau, R. F., Generation of strain waves in rock by an explosion in a spherical cavity, J. Geophys. Res., 74, 4267-4280, 1969.

Filson, J., C. W. Frasier, Multisite estimation of explosive source parameters, J. Geophys. Res., 77, 2045-2061, 1972.

Frasier, C. W., Observations of pP in the short-period phases of NTS explosions recorded at Norway, Geophys. J. R. Astr. Soc., 31, 99-109, 1972.

Fuchs, K., The transfer function for P-waves for a system consisting of a point source in a layered medium, Bull. Seism. Soc. Am., 56, 75-108, 1966.

Hasegawa, H. S., Analysis of teleseismic signals from underground nuclear explosions originating in four geological environments, Geophys. J. R. Astr. Soc., 24, 365-381, 1971.

Haskell, N. A., Analytic approximation for the elastic radiation from a contained underground explosion, J. Geophys. Res., 72, 2583-2587, 1967.

Helmberger, D. V., D. G. Harkrider, Seismic source descriptions of underground explosicns and a depth discriminate, Geophys. J. R. Astr. Soc., 31, 45-66, 1972.

Holzer, F., Calculation of seismic source mechanisms, Proc. Roy. Soc. London, A290, 408-429, 1966.

Honda, H., The elastic waves generated from a spherical source, Tokoku Univ. Sci. Rpts., Ser. 5, 11, 178-183, 1960.

Jeffreys, H., On the cause of oscillatory movement in seismograms, Mon. Not. R. Astr. Soc., Geophys. Suppl., 2, 407-416, 1931.

King, C. Y., W. H. Bakun, J. N. Murdock, Source parameters of nuclear explosions MILROW and LONGSHOT from teleseismic P waves, Geophys. J. R. Astr. Soc., 31, 27-44, 1972.

Kulhanek, O., P-wave amplitude spectra of Nevada underground nuclear explosions, Pure Appl. Geophys., 88, 121-136, 1971.

Lambert, D. G., E. A. Flinn, C. B. Archambeau, A comparative study of the elastic wave radiation from earthquakes and underground explosions, Geophys. J. R. Astr. Soc., 29, 403-432, 1972.

Melosh, H. J., Acoustic fluidization: A new geologic process?, J. Geophys. Res., 84, 7513-7520, 1979.

Molnar, P., P wave spectra from underground nuclear explosions, Geophys. J. R. Astr. Soc., 23, 273-287, 1971.

Mueller, R. A., J. R. Murphy, Seismic characteristics of underground nuclear detonations, Bull. Seism. Soc. Am., 61, 1675-1692, 1971.

Murphy, J. R., Seismic source functions and magnitude determinations for underground nuclear detonations, Bull. Seism. Soc. Am., 67, 135-158, 1977.

Peppin, W. A., P-wave spectra of Nevada Test Site events at near and very near distances: Implications for a near-regional body wave-surface wave discriminant, Bull. Seism. Soc. Am., 66, 803-825, 1976.

Perret, W. R., Close-in ground motion from the MILROW and CANNIKIN events, Bull. Seism. Soc. Am., 62, 1489-1504, 1972.

Press, F., C. B. Archambeau, Release of tectonic strain of underground nuclear explosions, J. Geophys. Res., 67, 337-343, 1962.

Rodean, H. C., Nuclear Explosion Seismology, U. S. Atomic Energy Commission, 156 p, 1971.

Sharpe, J. A., Production of elastic waves by explosion pressures, Geophysics, 7, 144-154, 1942.

Springer, D. L., Secondary sources of seismic waves from underground nuclear explosions, Bull. Seism. Soc. Am., 64, 581-594, 1974.

Stump, B. W., L. R. Johnson, The determination of source properties by the linear inversion of seismograms, Bull. Seism. Soc. Am., 67, 1489-1502, 1977.

Stump, B. W., Investigation of seismic sources by the linear inversion of seismograms, Ph.D. Thesis, University of California, Berkeley, 1979.

Thiruvenkatachar, V. R., K. Viswanathan, Dynamic response of an elastic half-space to time dependent surface tractions over an embedded spherical cavity, Proc. Roy. Soc., A287, 549-567, 1965.

Thiruvenkatachar, V. R., K. Viswanathan, Dynamic response of an elastic half-space to time dependent surface tractions over an embedded spherical cavity III, Proc. Roy. Soc., A309, 313-329, 1969.

Toksoz, M. N., K. C. Thompson, T. J. Ahrens, Generation of seismic waves by explosions in prestressed media, Bull. Seism. Soc. Am., 61, 1589-1623, 1971.

Toksoz, M. N., H. H. Kehrer, Tectonic strain release by underground nuclear explosions and its effect on seismic discrimination, Geophys. J. R. Astr. Soc., 31, 141-161, 1972.

Viecelli, J. A., Spallation and the generation of surface waves by an underground explosion, J. Geophys. Res., 78, 2475-2487, 1973.

von Seggren, D., R. Blandford, Source time functions and spectra of underground nuclear explosions, Geophys. J. R. Astr. Soc., 31, 83-97, 1972.

Werth, G. C., R. F. Herbst, D. L. Springer, Amplitudes of seismic arrivals from the M discontinuity, J. Geophys. Res., 67, 1587-1610, 1962.

Werth, G. C., R. F. Herbst, Comparison of amplitudes of seismic waves from nuclear explosions in four mediums, J. Geophys. Res., 68, 1463-1475, 1963.

Wyss, M., T. C. Hanks, R. C. Liebermann, Comparison of P-wave spectra of underground explosions and earthquakes, J. Geophys. Res., 76, 2716-2729, 1971.

V. Archival of Digital Seismic Data

A catalog has been assembled for most of the digital data which we have collected over the years in the process of conducting research sponsored by DARPA. Each entry in the catalog consists of a set of data which have been obtained by digitizing a portion of a seismogram or a suite of seismograms that were recorded from a particular seismic event. Most of the events in the catalog are explosions or earthquakes recorded at local or regional distances by seismographic stations in California, Nevada, and Utah, although a few events recorded at teleseismic distances are also included. The present catalog contains about 200 entries arranged in chronological order for the time period August 1965 to November 1971.

The digital data are now stored on punched cards in a binary format, and the possibility of putting the data on digital magnetic tape is being considered. Plans call for the time period covered by the catalog to be extended from 1971 up to the present. We also plan to put the index to the catalog in a computer where it can be accessed by a text editor and thus ease the task of updating the index.

The following pages contain the first version of the catalog index. It contains the information that was readily available in a first pass through the raw data files. Considerable more information about the digital data is available in various reports and records.

What follows is a brief explanation of the information which is contained in the index of the digital data catalog.

DATE - Date of the seismic event.

EVENT - Type of seismic event.

- EQ - Earthquake.
- EX - Nuclear explosion.
- C - Collapse of a nuclear explosion.
- EXA - Event following a nuclear explosion which is not identified as a collapse.
- BLAST - Chemical explosion.

STA. - Seismic station which recorded the event.

- JAS - Jamestown, California (U.C. Berkeley network).
- BRK - Berkeley, California (U.C. Berkelely network).
- PRI - Priest, California (U.C. Berkeley network).
- MMG - Mina, Nevada (LLNL network).
- EMG - Elko, Nevada (LLNL network).
- KMG - Kanab, Utah (LLNL network).
- LMG - Landers, California (LLNL network).
- BEFL - Belleview, Florida (LRSM network).
- HNME - Houlton, Maine (LRSM network).
- KNUT - Kanab, Utah (LRSM network).

LCNM - Las Cruces, New Mexico (LRSM network).

RKON - Red Lake, Ontario (LRSM network).

SJTX - San Jose, Texas (LRSM network).

TIME - Approximate origin time of event (hours, minutes GMT).

INST. - Type of instrument used to record the event.

BBV - Broad band velocity (see Peppin and McEvilly, Geophys. J. R. Astr. Soc., 37, 227-243, 1974).

SP - Short period.

FBA - Force-balance accelerometer.

COMPONENTS - Component of ground motion and other information.

Z - Vertical.

L - Longitudinal with respect to source direction.

T - Transverse with respect to source direction.

SM - Strong motion, low gain.

P - P wave arrival.

ℓ - Leader (recorded immediately preceding the event).

COMMENTS - Any other available information about the event.

DIGITAL DATA CATALOG

DATE	EVENT	STA.	TIME	INST.	COMPONENTS	COMMENTS
20 Aug 65	EQ Tonga Trench	BRK	2121	BBV	Z, Zℓ, L, Lℓ	22.9°S, 176.3°W, m_b 5.7
21 Sept 65	EQ Ryukyu	BRK	0138	BBV	Z, Zℓ, L, Lℓ	29.1°N, 129.2°E m_b 5.9
1 Oct 65	EQ Fiji Trench	BRK	1322	BBV	Z×2, Zℓ×2, L, Lℓ	20.0°S, 174.4°E m_b 5.7
25 Oct 65	EQ Kurile Is.	BRK	2234	BBV	Z, Zℓ, L, Lℓ	44.2°N, 145.3°E m_b 5.9
29 Oct 65	EX LONGSHOT	RKON		SP		
29 Oct 65	EX LONGSHOT	LCNM		SP		
29 Oct 65	EX LONGSHOT	JAS		SP	Z, Zℓ	
29 Oct 65	EX LONGSHOT	PRI		SP	Z, Zℓ	
29 Oct 65	EX LONGSHOT	BRK		BBV	Z, Zℓ	
3 Nov 65	EQ Peru - Bolivia	BRK	0139	BBV	Zℓ, Lℓ	9.1°S, 71.4°W M_b 6.0
13 Nov 65	EQ	JAS		SP	Z, Zℓ	
13 Nov 65	EQ	BRK		BBV	Z, Zℓ	
3 Feb 66	EX PLAID II	JAS		SP	(Z)ℓ	
6 Apr 66	EX STUTZ	JAS		SP	(Z)ℓ	
1 May 66	EQ Peru	BRK	1622	BBV	Z, Zℓ, L, Lℓ	8.5°S, 74.3°W m_b 5.6

DIGITAL DATA CATALOG

DATE	EVENT	STA.	TIME	INST.	COMPONENTS	COMMENTS
19 May 66	EX DUMONT	BRK	1356	BBV	Z, Zℓ, T, Tℓ, ZP, ZPℓ	
19 May 66	C DUMONT	BRK	1537	BBV	Z, Zℓ, T, Tℓ, ZP, ZPℓ	
28 June 66	EQ Parkfield F/S	BRK	0408	BBV	ZSMℓ, TSMℓ	
28 June 66	EQ Parkfield M/S	BRK	0426	BBV	ZSM, ZSMℓ, TSM, TSMℓ	
29 June 66	EQ * Parkfield A/S	BRK	1953	BBV	ZSMℓ, TSMℓ	
30 June 66	EQ * Parkfield A/S	BRK	0117	BBV	Z, Zℓ, T, Tℓ	
30 June 66	EX HALFBEAK	BRK	2215	BBV	ZSM, ZSMℓ, TSM, TSMℓ, ZP, ZPℓ	
1 July 66	C HALFBEAK	BRK	0133	BBV	Z, Zℓ, T, Tℓ, ZP, ZPℓ	
12 Sept 66	EX DERRINGER	JAS		SP	Z, Zℓ	
12 Sept 66	EX DERRINGER	BRK		BBV	Z, Zℓ, L, Lℓ	
7 Oct 66	EQ New Hebrides	BRK	1555	BBV	Z, Zℓ, L, Lℓ	21.6°S, 170.5°E mb 5.5
27 Oct 66	EQ Parkfield A/S	JAS	1206	SP	Z, Zℓ	
27 Oct 66	EQ Parkfield A/S	BRK	1206	BBV	Z, Zℓ	
27 Oct 66	EQ Parkfield A/S		1206		Z	
27 Oct 66	EQ Parkfield A/S	BRK	1206	BBV	Zℓ, T, Tℓ	
	* See 27 Oct 66 for another Parkfield A/S					

DIGITAL DATA CATALOG

DATE	EVENT	STA.	TIME	INST.	COMPONENTS	COMMENTS
20 Dec 66	EX GREELEY	BRK		BBV	ESM, ESMℓ, TSM, TSMℓ	
18 Jan 67	EQ	BRK		BBV	Z, Zℓ	
18 Jan 67	EQ	JAS		SP	Z, Zℓ	
19 Jan 67	EQ Fiji Trench	BRK	1240	BBV	Z, Zℓ, L, Lℓ	14.8° S, 178.8° W mb 6.7
20 Jan 67	EQ	BRK	0209	BBV	Z, Zℓ	
20 Jan 67	EQ	JAS	0209	SP	Z, Zℓ	
15 Feb 67	EQ Peru - Bolivia	BRK	1611	BBV	Zℓ, Lℓ	9.0° S, 71.3° W mb 6.5
23 Feb 67	EX AGILE	BRK	1850	BBV	Z, Zℓ, T, Tℓ, ZP, ZPℓ	
23 Feb 67	C AGILE	BRK	2111	BBV	Z, Zℓ, T, Tℓ, ZP, ZPℓ	
26 Feb 67	EQ	JAS		SP	Z, Zℓ	
27 Apr 67	EX EFFENDI	JAS		SP	(Z), (Z)ℓ	
28 Apr 67	EQ	JAS		SP	(Z), (Z)ℓ	
7 May 67	EQ	JAS		SP	(Z), (Z)ℓ	
23 May 67	EX SCOTCH	BRK	1400	BBV	Z, Zℓ, T, Tℓ, ZP, ZPℓ	

DIGITAL DATA CATALOG

DATE	EVENT	STA.	TIME	INST.	COMPONENTS	COMMENTS
23 May 67	EXA SCOTCH	JAS	2014	SP	Z, Zℓ	
23 May 67	EXA SCOTCH	BRK	2014	BBV	Z, Zℓ, T, Tℓ, ZPℓ	
29 June 67	EX UMBER	JAS		SP	(Z)ℓ	
29 July 67	EQ	BRK		BBV	Z, Zℓ, L, Lℓ	
10 Aug 67	EX WASHER	JAS		SP	Z, (Z)ℓ	
13 Aug 67	EQ Honshu	BRK	2006	BBV	Z, Zℓ, L, Lℓ	35.3°N, 135.3°E, M6 6.4
24 Aug 67	EQ	JAS		SP	(Z), (Z)ℓ	
7 Sept 67	EX YARD	BRK	1345	BBV	Z, Zℓ, T, Tℓ, ZP, ZPℓ	
7 Sept 67	C YARD	BRK	1424	BBV	Z, Zℓ, T, Tℓ, ZP, ZPℓ	
9 Oct 67	EQ Tonga Trench	BRK	1721	BBV	Z, Zℓ, L, Lℓ, ZSM	21.1°S, 179.3° W M6 6.9
27 Dec 67	EQ Chile Bolivia	BRK	0917	BBV	Z, Zℓ, L, Lℓ	21.2° S, 68.3° W M6 6.8
18 Jan 68	EX HUPMOBILE	JAS		SP	Z, (Z)ℓ	
26 Jan 68	EX CABRIOLET	JAS		SP	Z, (Z)ℓ	
29 Jan 68	EQ Hokkaido	BRK	1019	BBV	L, Lℓ, L, Lℓ	43.6°N, 146.7° E M6 7.1
21 Feb 68	EX KNOX	BRK	1530	BBV	Z, Zℓ, T, Tℓ, ZP, ZPℓ	

DIGITAL DATA CATALOG

DATE	EVENT	STA.	TIME	INST.	COMPONENTS	COMMENTS
21 Feb 68	C KNOX	BRK	1634	BBV	Z, Z$_L$, T, T$_L$, ZP, ZP$_L$	
11 Mar 68	EQ Tonga Trench	BRK	0826	BBV	Z, Z$_L$, L, L$_L$	16.2° S, 173.9° W mb 6.0
12 Mar 68	Ex BUGGY I	JAS		SP	Z, (?)$_L$	
1 Apr 68	EQ Kyushu	BRK	0042	BBV	Z, Z$_L$, L, L$_L$	32.5° N, 132.2° E mb 7.1
9 Apr 68	EQ Borrego	BRK	0230	BBV	ZSM, ZSM$_L$, TSM, TSM$_L$	
9 Apr 68	EQ Borrego AIS	BRK	0303	BBV	Z, Z$_L$, T, T$_L$	
23 Apr 68	Ex SCROLL	JAS		SP	Z, Z$_L$	
24 Apr 68	Ex BOXCAR	BRK	1500	BBV	ZSM, ZSM$_L$, TSM, TSM$_L$, ZPSM, ZPSM$_L$	
26 Apr 68	Ex A, I BOXCAR	BRK	1532	BBV	Z, Z$_L$, T, T$_L$, ZP, ZP$_L$	
24 Apr 68	C, II BOXCAR	BRK	1634	BBV	Z, Z$_L$, T, T$_L$, ZP, ZP$_L$	
16 May 68	EQ Hokkaido	BRK	0048	BBV	Z, Z$_L$, L, L$_L$	40.8° N, 143.2° E mb 6.8
17 May 68	Ex CLARKSMOBILE	JAS	1300	SP	Z	
17 May 68	Ex CLARKSMOBILE	PRI	1300	SP	Z, Z$_L$	
17 May 68	C CLARKSMOBILE	JAS		SP	Z, (?)$_L$	
22 May 68	EQ Central Nevada	JAS	1321	SP	Z, (?)$_L$	

DIGITAL DATA CATALOG

DATE	EVENT	STA.	TIME	INST.	COMPONENTS	COMMENTS
22 May 68	EQ Central Nevada	BRK	1321	BBV	Z, Ze, T, Te, ZP, ZPe	
28 May 68	EQ Adel, Oregon	BRK	1255	BBV	Z, Ze, T, Te, ZP, ZPe	
30 May 68	EQ Adel, Oregon	BRK	0055	BBV	Z, Ze, T, Te, ZP, ZPe	
16 June 68	EQ North Nevada	BRK	1402	BBV	Z, Ze, T, Te, ZP, ZPe	
19 June 68	EQ Peru-Ecuador	BRK	0813	BBV	Z, Ze, L, Le	5.6°S, 77.2° W m_b 6.7
29 June 68	EQ Santa Barbara F/S I	BRK	1912	BBV	Z, Ze, T, Te, ZP, ZPe	
29 June 68	EQ Santa Barbara F/S II	BRK	2035	BBV	Z, Ze, T, Te, ZP, ZPe	
5 July 68	EQ Santa Barbara F/S III	BRK	0056	BBV	Z, Ze, T, Te, ZP, ZPe	
5 July 68	EQ Santa Barbara m/s (#4)	BRK	0045	BBV	ZSM, ZSMe, TSM, TSMe, ZP ZPe	
7 July 68	EQ Santa Barbara A/S	BRK	1433	BBV	Z, Ze, T, Te, ZP, ZPe	
30 July 68	EX TANITH	JAS		SP	Z, (E)e	
2 Aug 68	EQ	BRK		BBV	ZSM, ZSMe, LSM, LSMe	
5 Aug 68	EQ Kyushu	BRK	1617	BBV	Z, Ze, L, Le	33.3° N, 132.2° E m_b 6.4
25 Sept 68	EQ	BRK		BBV	Z, Ze, L, Le	

DIGITAL DATA CATALOG

DATE	EVENT	STA.	TIME	INST.	COMPONENTS	COMMENTS
22 Nov 68	EX TINDERBOX	JAS		SP	Z, (?)	
19 Dec 68	EX BENHAM	BRK	1630	BBV	ZSM, ZSMℓ, TSM, TSMℓ, ZPSM, ZPSMℓ	
19 Dec 68	C BENHAM A/S I	BRK	2224	BBV	Z, Zℓ, T, Tℓ, ZP, ZPℓ	
21 Dec 68	EXA BENHAM A/S II	JAS	0014	SP	Z, (E)ℓ	
21 Dec 68	EXA BENHAM A/S II	BRK	0014	BBV	Z, Zℓ, T, Tℓ, ZP, ZPℓ	
21 Dec 68	EXA BENHAM A/S II	MMG	0014	BBV	Z, Zℓ	
21 Dec 68	EXA BENHAM A/S II	KMG	0014	BBV	Z, Zℓ	
21 Dec 68	EXA BENHAM A/S II	LMG	0014	BBV	Z, Zℓ	
22 Dec 68	EXA BENHAM A/S III	BRK	1810	BBV	Z, Zℓ, T, Tℓ, ZP, ZPℓ	
6 Jan 69	EXA BENHAM A/S	JAS	0634	SP	Z, Zℓ	
6 Jan 69	EXA BENHAM A/S	BRK	0634	BBV	Z, Zℓ, T, Tℓ, ZP, ZPℓ	
6 Jan 69	EXA BENHAM A/S	LMG	0634	BBV	Z, Zℓ	
6 Jan 69	EXA BENHAM A/S	MLG	0634	BBV	Z, Zℓ	
6 Jan 69	EXA BENHAM A/S	KMG	0634	BBV	Z, Zℓ	

DIGITAL DATA CATALOG

DATE	EVENT	STA.	TIME	INST.	COMPONENTS	COMMENTS
10 Jan 69	EXA BENHAM A/S IV	BRK	0941	BBV	Z, Ze, T, Te, ZP, ZP.C	
10 Jan 69	EXA BENHAM A/S IV	MMG	0941	BBV	Z, Ze	
10 Jan 69	EXA BENHAM A/S IV	LMG	0941	BBV	Z, Ze	
10 Jan 69	EXA BENHAM A/S V	JAS	1701	SP	Z, (Z)e	
10 Jan 69	EXA BENHAM A/S V	BRK	1701	BBV	Z, Ze, T, Te, ZP, ZP.C	
10 Jan 69	EXA BENHAM A/S VI	JAS	1714	SP	Z, (Z)e	
10 Jan 69	EXA BENHAM A/S VI	BRK	1714	BBV	Z, Ze, T, Te, ZP, ZP.C	
15 Jan 69	EX PACKARD	JAS	1900	SP	(Z), Ze	
15 Jan 69	EX PACKARD	PRI	1900	SP	(Z), (Z)e	
15 Jan 69	EX WINESKIN	JAS	1930	SP	(Z), Ze	
15 Jan 69	EX WINESKIN	PRI	1930	SP	(Z), Ze	
15 Jan 69	C PACKARD & WINESKIN	JAS	2013	SP	(Z), (Z)e	
19 Jan 69	EQ Hokkaido	BRK	0702	BBV	Z, Ze, L, Le	45.0° N, 143.2° E mb 7.0
22 Jan 69	EQ	JAS		SP	(Z), (Z)e	
30 Jan 69	EX LISE	JAS		SP	(Z), Ze	
	EX	PRI		SP	(Z), Ze	

DIGITAL DATA CATALOG

DATE	EVENT	STA.	TIME	INST.	COMPONENTS	COMMENTS
10 Feb 69	EQ Tonga - Fiji	BRK	2258	BBV	ZSM, Z, Zℓ, L, Lℓ	22.7°S, 178.6°E Mb 6.5
12 Feb 69	EX CYPRESS	JAS		SP	(Z), Zℓ	
12 Feb 69	EX CYPRESS	PRI		SP	(Z), (Z)ℓ	
28 Feb 69	EQ Gibraltar	BRK	0240	BBV	ZSM, ZSMℓ, LSM, LSMℓ	36.0°N, 10.6°W Mb 8.3
20 Mar 69	EX BARSAC	JAS	1813	SP	(Z), Zℓ	
20 Mar 69	EX BARSAC	PRI	1813	SP	(Z), Zℓ	
21 Mar 69	EX COFFER	JAS	1430	SP	(Z), Zℓ	
21 Mar 69	EX COFFER	PRI	1430	SP	(Z), (Z)ℓ	
31 Mar 69	EQ Honshu	BRK	1925	BBV	Z, Zℓ, L, Lℓ	38.3°N, 134.6°E Mb 5.9
16 Sept 69	EX JORUM	Temporary Network	1430	FBA	Z2, Z2ℓ, Z3, Z3ℓ, Z4, Z4ℓ, Z5, Z5ℓ, Z6, Z6ℓ, T1×2,	High gain data
					T1ℓ, T2, T2ℓ, T3, T3ℓ, T4, T4ℓ, T5, T5ℓ, T6, T6ℓ	
16 Sept 69	EX JORUM	BRK	1430	BBV	ZPSM, ZPSMℓ, ZSM, ZSMℓ, TSM, TSMℓ	
16 Sept 69	(C) JORUM AFS	Temporary Network	1442	FBA	Z1, Z1ℓ, Z2, Z2ℓ, Z3, Z3ℓ, Z4, Z4ℓ, Z5, Z5ℓ, Z6, Z6ℓ, T1,	
					T1ℓ, T2, T2ℓ, T3, T3ℓ, T4, T4ℓ, T5, T5ℓ, T6, T6ℓ	

DIGITAL DATA CATALOG

DATE	EVENT	STA.	TIME	INST.	COMPONENTS	COMMENTS
16Sept69	(C) JORUM AIS	Temporary Network	1505	FBA	Z1, Z1L, Z2, Z2L, Z3, Z3L, Z4, Z4L, Z5, Z5L, Z6, Z6L, T1,	
					T1L, T2, T2L, T3, T3L, T4, T4L, T5, T5L, T6, T6L	
16Sept69	(C) JORUM AIS	Temporary Network	1515	FBA	Z1, Z1L, Z2, Z2L, Z3, Z3L, T1, T1L, T2, T2L, T3, T3L	
16Sept69	(C) JORUM AIS	Temporary Network	1516	FBA	Z1, Z2, Z3, Z4, Z4L ×2, Z5, Z5L ×2, Z6, Z6L ×2, T1, T2,	
					T3, T4, T4L ×2, T5, T5L ×2, T6, T6L ×2	
(16Sept69)	(C) JORUM AIS	Temporary Network	1531	FBA	Z1, Z1L, Z2, Z2L, Z3, Z3L, T1, T1L, T2, T2L, T3, T3L	
(16Sept69)	(C) JORUM AIS		1532		Z4, Z4L, Z5, Z5L, Z6, Z6L, T4, T4L, T5, T5L, T6, T6L	
16Sept69	C JORUM AIS	BRK	1544	BBV	Z, ZL, T, TL, ZP, ZPL	68
16Sept69	C JORUM AIS	Temporary Network	1544	FBA	Z1, Z1L, Z2, Z2L, Z3, Z3L, Z4, Z4L, Z5, Z5L, Z6, Z6L,	
					T1, T1L, T2, T2L, T3, T3L, T4, T4L, T5, T5L, T6, T6L	
(16Sept69)	(C) JORUM AIS	Temporary Network	1602	FBA	Z1, Z1L, Z2, Z2L, Z3, Z3L T1, T1L, T2, T2L, T3, T3L	
(16Sept69)	(C) JORUM AIS		1603		Z4L, Z5L, Z6L, T4L, T5L, T6L	
(16Sept69)	(C) JORUM AIS	Temporary Network	1607	FBA	Z1, Z1L, Z2, Z2L, Z3, Z3L, T1, T1L, T2, T2L, T3, T3L	
16Sept61	C JORUM AIS	BRK	1623	BBV	Z, ZL, T, TL, ZP, ZPL	
16Sept69	C JORUM AIS	JAS	1623	SP	ZP, ZPL	

DIGITAL DATA CATALOG

DATE	EVENT	STA.	TIME	INST.	COMPONENTS	COMMENTS
(16Sept69)	(C) JORUM A/S	Temporary Network	1656	FBA	Z1, Z1L, Z2, Z2L, Z3, Z3L, T1, T1L, T2, T2L, T3, T3L	
(16Sept69)	(C) JORUM A/S	Temporary Network	1717	FBA	Z1, Z1L, Z2, Z2L, Z3, Z3L, T1, T1L, T2 T2L, T3, T3L	
16Sept69	C JORUM A/S	BRK	1731	BBV	E, EL, T, TL, EP, EPL	
16Sept69	C JORUM A/S	Temporary Network	1731	FBA	Z1, Z1L, Z2, Z2L, Z3, Z3L, Z4, Z4L, Z5, Z5L, Z6, Z6L	
					T1, T1L, T2, T2L, T3, T3L, T4, T4L, T5, T5L, T6, T6L	
16Sept69	C JORUM A/S	BRK	1815	BBV	E, EL, T, TL, EP, EPL	
16Sept69	C JORUM A/S	Temporary Network	1815	FBA	Z1, Z1L, Z2, Z2L, Z3, Z3L, Z4, Z4L, Z5, Z5L	
					T1, T1L, T2, T2L, T3, T3L, T4, T4L, T5, T5L, T6, T6L	
(16Sept69)	(C) JORUM A/S	Temporary Network	1928	FBA	Z1L, Z2L, Z3, Z3L, Z4L, Z5, Z5L, Z6, Z6L, T1L T2L,	
					T3, T3L, T4L, T5, T5L, T6 x2, T6L x2	
20Oct69	EX MILROW	HNME		SP		
20Oct69	EX MILROW	KNUT		SP		
2 Oct69	EX MILROW	SJTX		SP		
2 Oct69	EX MILROW	LCNM		SP		
2 Oct69	EX MILROW	RKON		SP		

DIGITAL DATA CATALOG

DATE	EVENT	STA.	TIME	INST.	COMPONENTS	COMMENTS
8 Oct 69	EX PIPKIN	BRK	1430	BBV	Z, Zℓ, T, Tℓ, ZP, ZPℓ	
21 Oct 69	EQ Amchitka		2053		ZP, ZPℓ	
29 Oct 69	EX CRUET	LMG		BBV	Z, Zℓ	
29 Oct 69	EX CRUET	MMG		BBV	Z, Zℓ	
29 Oct 69	EX CRUET	KMG		BBV	Z, Zℓ	
31 Oct 69	EQ Amchitka		1133		ZP, ZPℓ	
13 Feb 70	BLAST	JAS		SP	Z, Zℓ	
16 Feb 70	BLAST	JAS		SP	Z, Zℓ	
17 Feb 70	BLAST	JAS		SP	Z, Zℓ	
18 Feb 70	BLAST	JAS		SP	Z, Zℓ	
27 Feb 70	EQ Amchitka		0708		ZP, ZPℓ	
26 Mar 70	EX HANDLEY	Temporary Network	1900	FBA	Z1 x2, Z1ℓ, Z2, Z2ℓ, Z3 x2, Z3ℓ, Z4, Z4ℓ, Z5, Z5ℓ,	High gain data
					T1, T1ℓ, T2, T2ℓ, T3, T3ℓ, T4, T4ℓ, T5, T5ℓ	
26 Mar 70	EX HANDLEY	BRK	1900	BBV	ZSM, ZSMA, TSM x2, TSMℓ	

DIGITAL DATA CATALOG

DATE	EVENT	STA.	TIME	INST.	COMPONENTS	COMMENTS
27 Mar 70	C HANDLEY A/S	Temporary Network	0552	FBA	Z1=3, Z1i, Z2, Z2i, T1, T1i, T2=2, T2i	
27 Mar 70	C HANDLEY A/S	Temporary Network	1643	FBA	Z1, Z1i, Z2, Z2i, Z3, Z3i, T1, T1i, T2 T2i, T3 T3i	
27 Mar 70	C HANDLEY A/S	Temporary Network	1808	FBA	Z3, Z3i, T3, T3i	
27 Mar 70	C or EXT HANDLEY A/S		1809		Z1, Z1i, Z2, Z2i, T1, T1i, T2, T2i	
27 Mar 70	C or EXT HANDLEY A/S	Temporary Network	1818	FBA	Z1i, Z2, Z2i, Z3, Z3i, T1, T1i, T2, T2i, T3, T3i	
27 Mar 70	(C) HANDLEY A/S		1952		Z4, Z4i, Z5, Z5i, T4, T4i, T5, T5i	
27 Mar 70	(C) HANDLEY A/S	Temporary Network	2010	FBA	Z1=2, Z1i, Z2=2, Z2i, Z4, Z4i, Z5, Z5i,	
					T1, T1i, T2, T2i, T4, T4i, T5, T5i	
27 Mar 70	(C) HANDLEY A/S	Temporary Network	2012	FBA	Z4, Z4i, Z5, Z5i, T4, T4i, T5i	
27 Mar 70	(C) HANDLEY A/S		2013		Z1, Z1i, Z2, Z2i, T1, T1i, T2, T2i, T5	
21 May 70	EX MORRONES	MMC		BBV	Z, Zi	
21 May 70	EX MORRONES	KMC		BBV	Z, Zi	
21 May 70	EX MORRONES	LMC		BBV	Z, Zi	

DIGITAL DATA CATALOG

DATE	EVENT	STA.	TIME	INST.	COMPONENTS	COMMENTS
9 Feb 71	EQ San Fernando	BRK		BBV	Z, Ze, T, Te, ZSM, ZSMe, TSM, TSMe	
					ZP, ZPe, ZPSM, ZPSMe	
10 Feb 71	EQ San Fernando Ms	BRK		BBV	Z, Ze, T, Te, ZP, ZPe	
5 Aug 71	EQ Massachusetts Mt.	KMG	1758	BBV	Z, Ze	36° 54.9' N, 115° 59.4' W M_L 4.2
5 Aug 71	EQ Massachusetts Mt.	LMG	1758	BBV	Z, Ze	
5 Aug 71	EQ Massachusetts Mt.	EMG	1758	BBV	Z, Ze	
5 Aug 71	EQ Massachusetts Mt.	JAS	2118	SP	Z	
5 Aug 71	EQ Massachusetts Mt.	JAS	2221	SP	Z	36° 53.6' N, 115° 56.3 W, M_L 3.3
8 Oct 71	EX CATHAY	EMG		BBV	Z, Ze	
8 Oct 71	EX CATHAY	KMG		BBV	Z, Ze	
8 Oct 71	EX CATHAY	LMG		BBV	Z, Ze	
8 Oct 71	EX CATHAY	MMG		BBV	Z, Ze	
6 Nov 71	EX CANNIKIN		2200		ZP, ZPe	
6 Nov 71	EX CANNIKIN	HNME		SP		
6 Nov 71	EX CANNIKIN	KNUT		SP		

72

DIGITAL DATA CATALOG

DATE	EVENT	STA.	TIME	INST.	COMPONENTS	COMMENTS
6 Nov 71	EX CANNIKIN	BRK		BBV		
6 Nov 71	EX CANNIKIN	SJTX		SP		
6 Nov 71	EX CANNIKIN	BEFL		SP		
6 Nov 71	EX CANNIKIN	RKON		SP		
6 Nov 71	EX CANNIKIN	PRI		SP	Z	